Lattice QCD and Pion Physics

Xu Feng (冯旭)

北京大学
PEKING UNIVERSITY

Hadron Physics Online Forum, 2020/10/09

Pion plays unique role in QCD and Nuclear theory

- First proposed by H. Yukawa in 1935 as carrier particles of the nuclear force

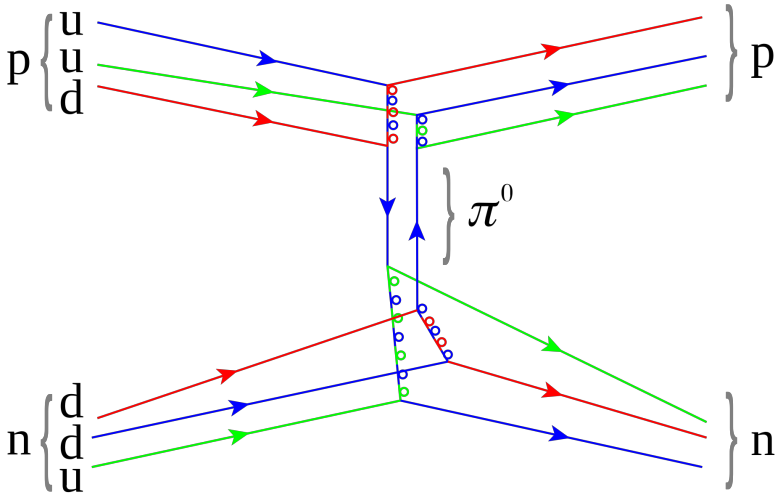

- Spontaneous chiral symmetry breaking discovered by Y. Nambu in 1960

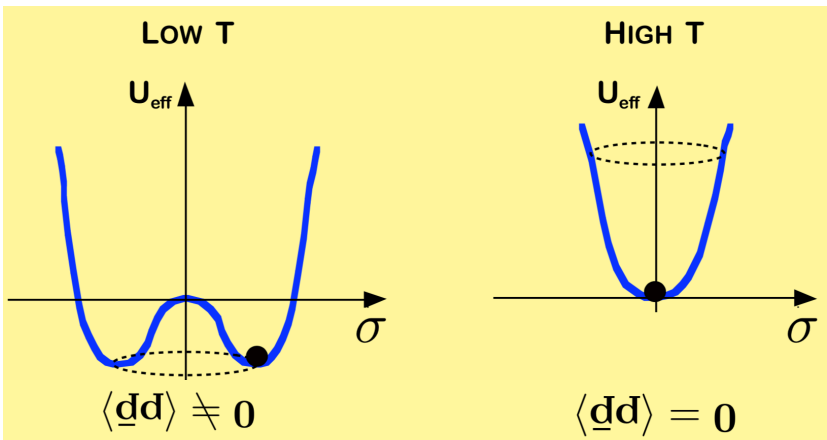

Pions are Nambu-Goldstone bosons for two-flavor SχSB

QCD: different strategies

QCD is the fundamental theory

$\Rightarrow$ describing strong interaction between quarks and gluons

- High-Q ($>$ few GeV) $\leftrightarrow$ short distance ($<$ 0.1 fm)
  $\Rightarrow$ Theory of weakly interacting quarks and gluons
  $\Rightarrow$ (Perturbative QCD: Gross, Politzer, Wilczek for asymptotic freedom)

- Low-Q ($\ll$ 1 GeV) $\leftrightarrow$ long distance ($>$ 1 fm)
  $\Rightarrow$ Spontaneous chiral symmetry breaking
  $\Rightarrow$ EFT of weakly interacting Nambu-Goldstone bosons (pions)

- Lattice QCD
  $\Rightarrow$ Large-scale supercomputer simulation on Euclidean spacetime lattice
  - Provide most accurate α_s for pQCD
  - Provide LECs for Chiral Perturbation Theory

Precision era for lattice QCD

Flavor Lattice Averaging Group (FLAG) average 2019

$$f_+^{K\pi}(0) = 0.9706(27) \quad \Rightarrow \quad 0.28\% \text{ error}$$

$$f_{K^\pm}/f_{\pi^\pm} = 1.1932(19) \quad \Rightarrow \quad 0.16\% \text{ error}$$

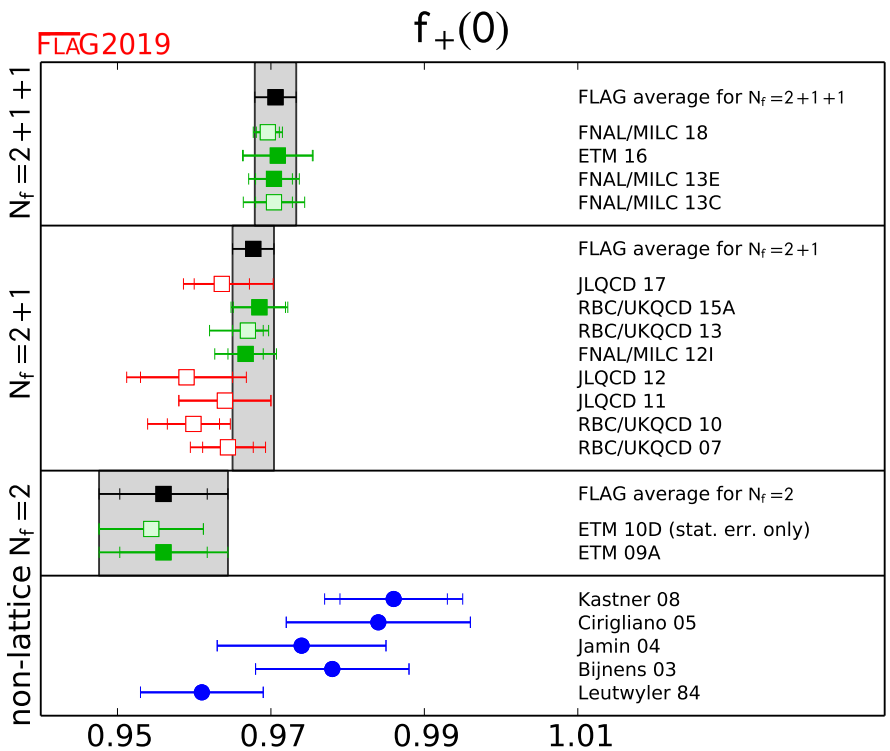

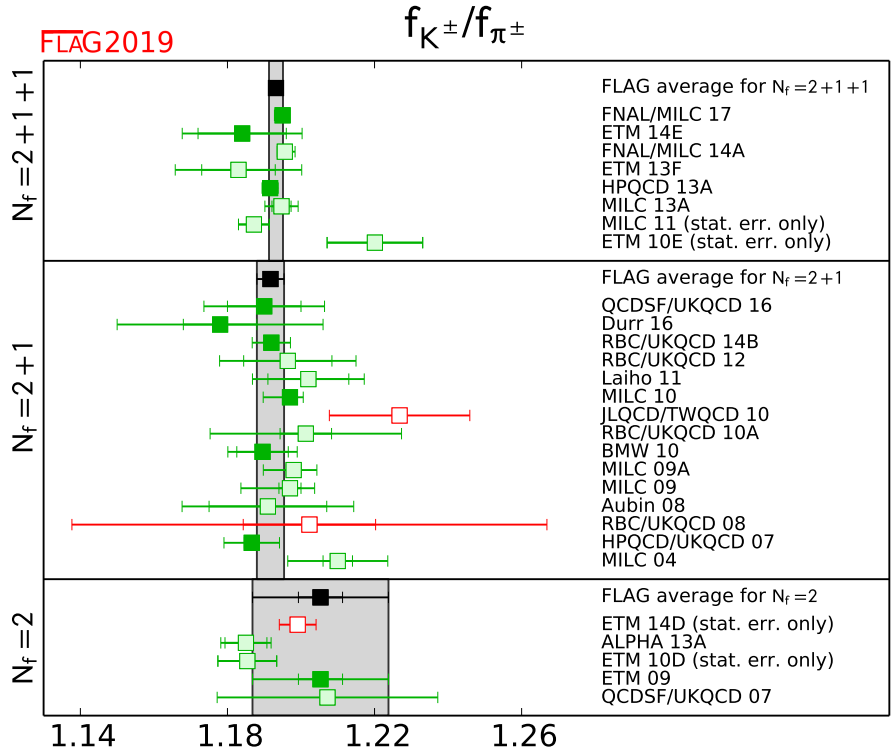

Experimental information [arXiv:1411.5252, 1509.02220]

$$K_{\ell 3} \quad \Rightarrow \quad |V_{us}| f_+(0) = 0.2165(4) \quad \Rightarrow \quad |V_{us}| = 0.2231(7)$$

$$K_{\mu 2}/\pi_{\mu 2} \quad \Rightarrow \quad \left|\frac{V_{us}}{V_{ud}}\right| \frac{f_{K^\pm}}{f_{\pi^\pm}} = 0.2760(4) \quad \Rightarrow \quad \left|\frac{V_{us}}{V_{ud}}\right| = 0.2313(5)$$

Flag average 2019

Error < 1%

	N_f	FLAG average	Frac. Err.
f_K/f_π	$2+1+1$	1.1932(19)	0.16%
$f_+(0)$	$2+1+1$	0.9706(27)	0.28%
f_D	$2+1+1$	212.0(7) MeV	0.33%
f_{D_s}	$2+1+1$	249.9(5) MeV	0.20%
f_{D_s}/f_D	$2+1+1$	1.1783(16)	0.13%
f_B	$2+1+1$	190.0(1.3) MeV	0.68%
f_{B_s}	$2+1+1$	230.3(1.3) MeV	0.56%
f_{B_s}/f_B	$2+1+1$	1.209(5)	0.41%

Error < 5%

	N_f	FLAG average	Frac. Err.
$\hat{B}_K$	$2+1$	0.7625(97)	1.3%
$f_+^{D\pi}(0)$	$2+1$	0.666(29)	4.4%
$f_+^{DK}(0)$	$2+1$	0.747(19)	2.5%
$\hat{B}_{B_s}$	$2+1$	1.35(6)	4.4%
B_{B_s}/B_{B_d}	$2+1$	1.032(28)	3.7%
...			

Precision beyond 1% $\Rightarrow$ time to include QED

Pion projects – outline of this talk

- QCD+QED ⇒ Pion mass splitting
  [XF, L. Jin, PRD100 (2019) 094509]
- Electroweak box contribution to $\pi_{\ell 3}$ decay
  [XF, M. Gorchtein, L. Jin, P. Ma, C. Seng, PRL124 (2020) 192002]
- Neutrinoless double beta decay of pion
  [XF, L. Jin, X. Tuo, S. Xia, PRL122 (2019) 022001]
  [X. Tuo, XF, L. Jin, PRD100 (2019) 094511]
- Pion charge radius
  [XF, Y. Fu, L. Jin, PRD101 (2020) 051502 (Rapid Communication)]

Here, Y. Fu, P. Ma, X. Tuo & S. Xia are PhD students from PKU

QCD+QED

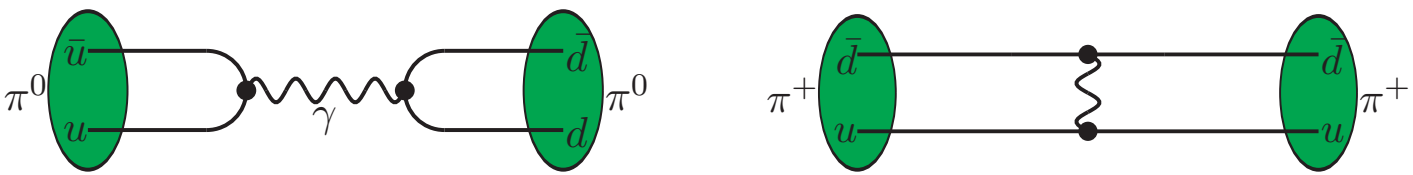

Long range photon on the lattice

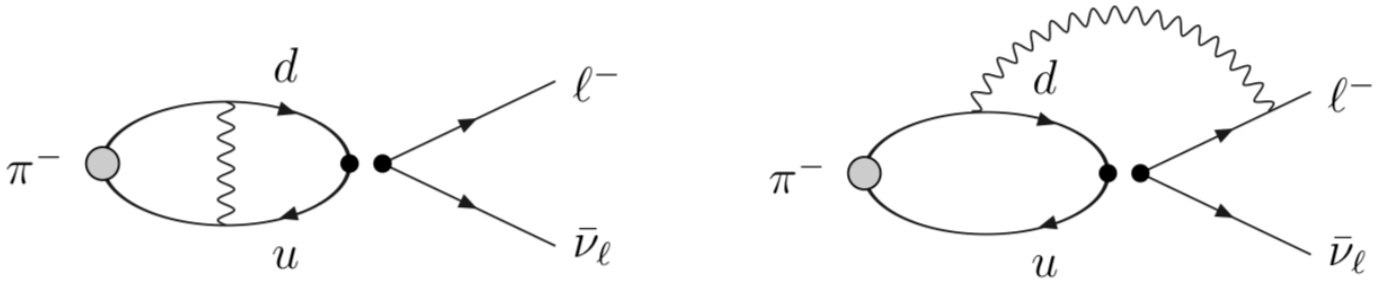

$m_\gamma = 0 \Rightarrow$ long-range propagator enclosed in the lattice box

$\Rightarrow$ power-law finite-size effects

Various methods proposed to treat photon on the lattice

- $\mathrm{QED_L}$ and $\mathrm{QED_{TL}}$ [Hayakawa & Uno, 2008; S. Borsany et. al., 2015]
- Massive photon [M. Endres et. al., 2016]
- C^* boundary condition [B. Lucini et. al., 2016]

Change photon propagators to make it suitable for lattice

Remove zero mode - $\mathrm{QED_L}$

Infinite volume propagator $\Rightarrow$ **finite-volume propagator**

$$S_\infty(x) = \int \frac{d^4p}{(2\pi)^4}\frac{e^{ipx}}{p^2} = \frac{1}{4\pi^2x^2} \quad \Rightarrow \quad S_L(x) = \frac{1}{VT}\sum_p{}' \frac{e^{ipx}}{p^2}, \quad p = \frac{2\pi}{L}n \neq 0$$

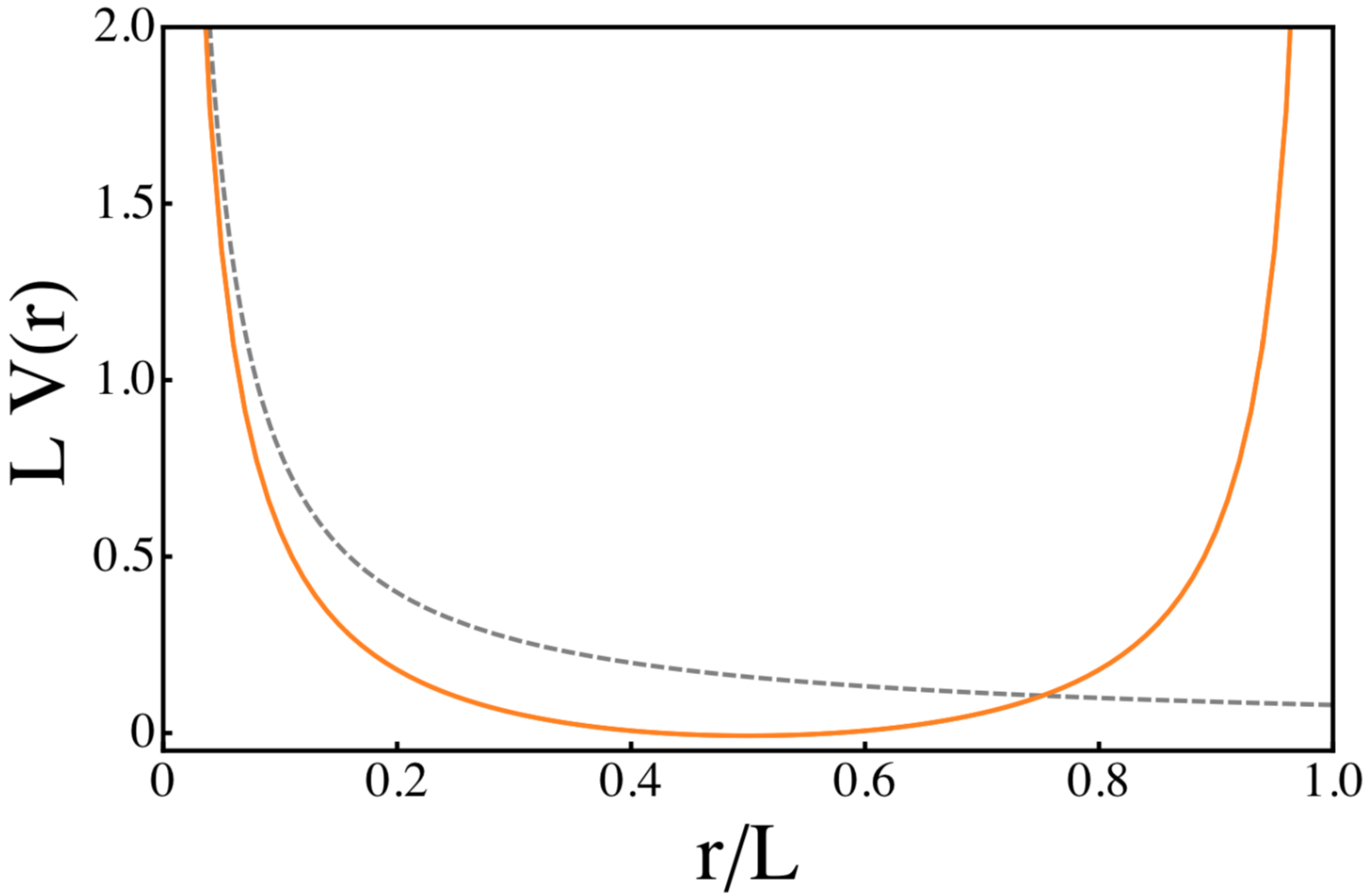

[Davoudi, Savage, PRD90 (2014) 054503]

Power-law $(1/L^n)$ finite volume effect as lattice volume L increase

QED self energy: pion mass splitting

$m_{\pi^+} - m_{\pi^0}$:

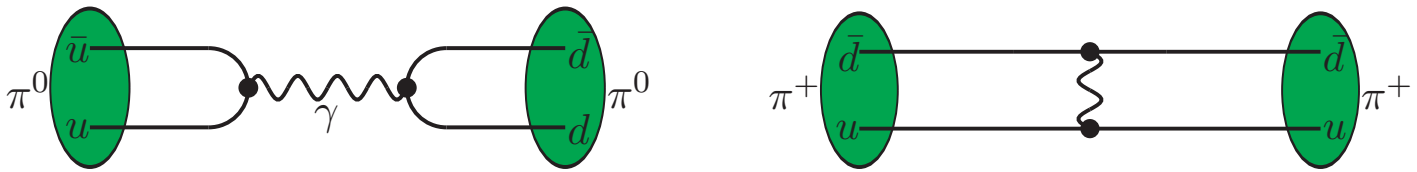

type 1 type 2

Isospin breaking effects: EM (α_e) + strong ($\frac{m_u - m_d}{\Lambda_{\rm QCD}}$) contributions

- Strong IB breaking appears at $O\left(\left(\frac{m_u - m_d}{\Lambda_{\rm QCD}}\right)^2\right)$ $\Rightarrow$ dominated by EM effect

Ideal testing ground to isolate the QED effects

- Previous calculation by [RM123 collaboration, 2013]

$$M^2_{\pi^+} - M^2_{\pi^0} = 1.44(13)_{\rm stat}(16)_{\rm chiral} \times 10^3 \ \text{MeV}^2$$

  - $O(1\%)$ precision
  - including type 2 diagram only

Infinite-volume reconstruction method

[XF, L. Jin, PRD100 (2019) 094509]

FV effects mimicking by scalar QED

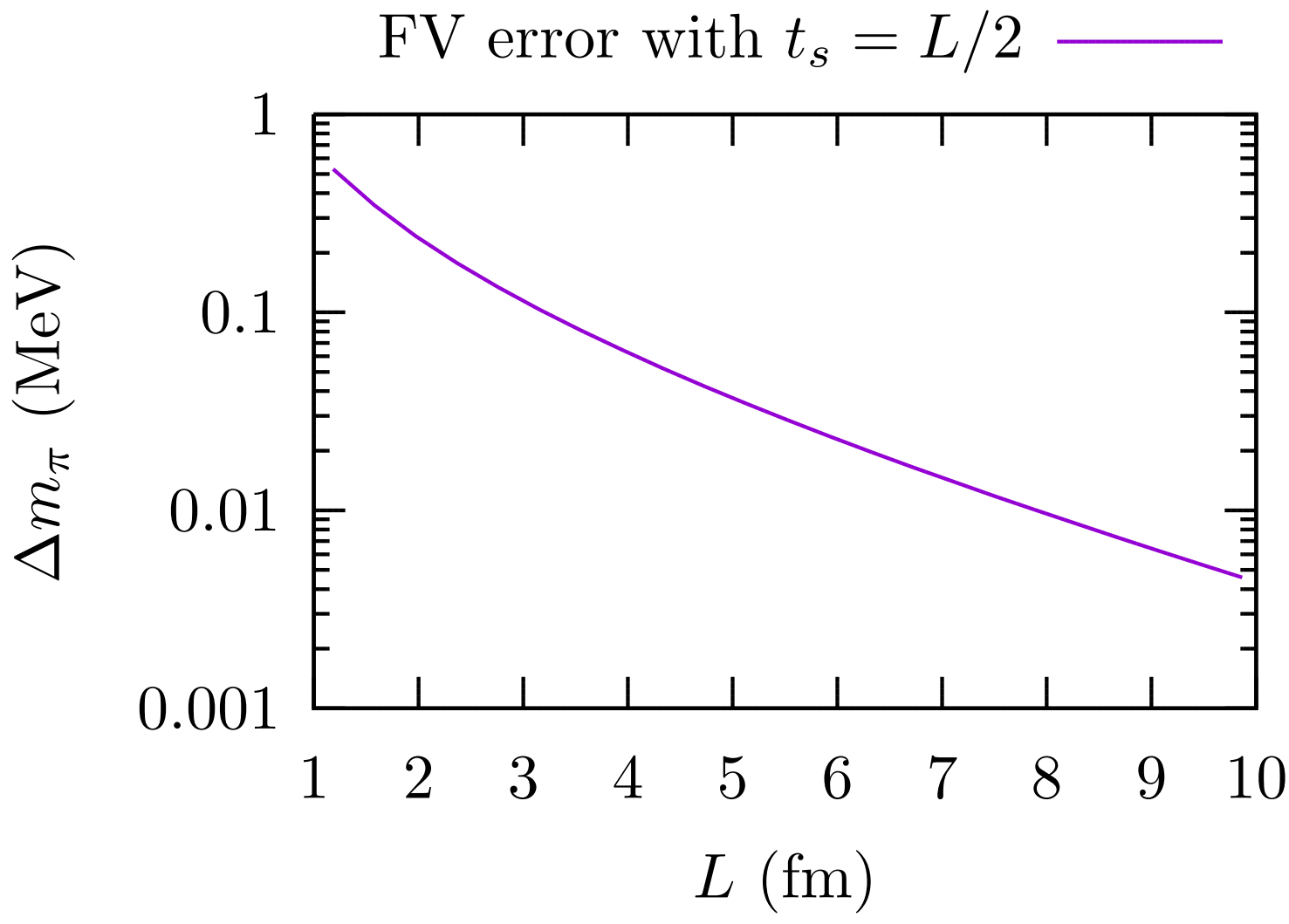

FV error exponentially suppressed

Using infinite-volume reconstruction

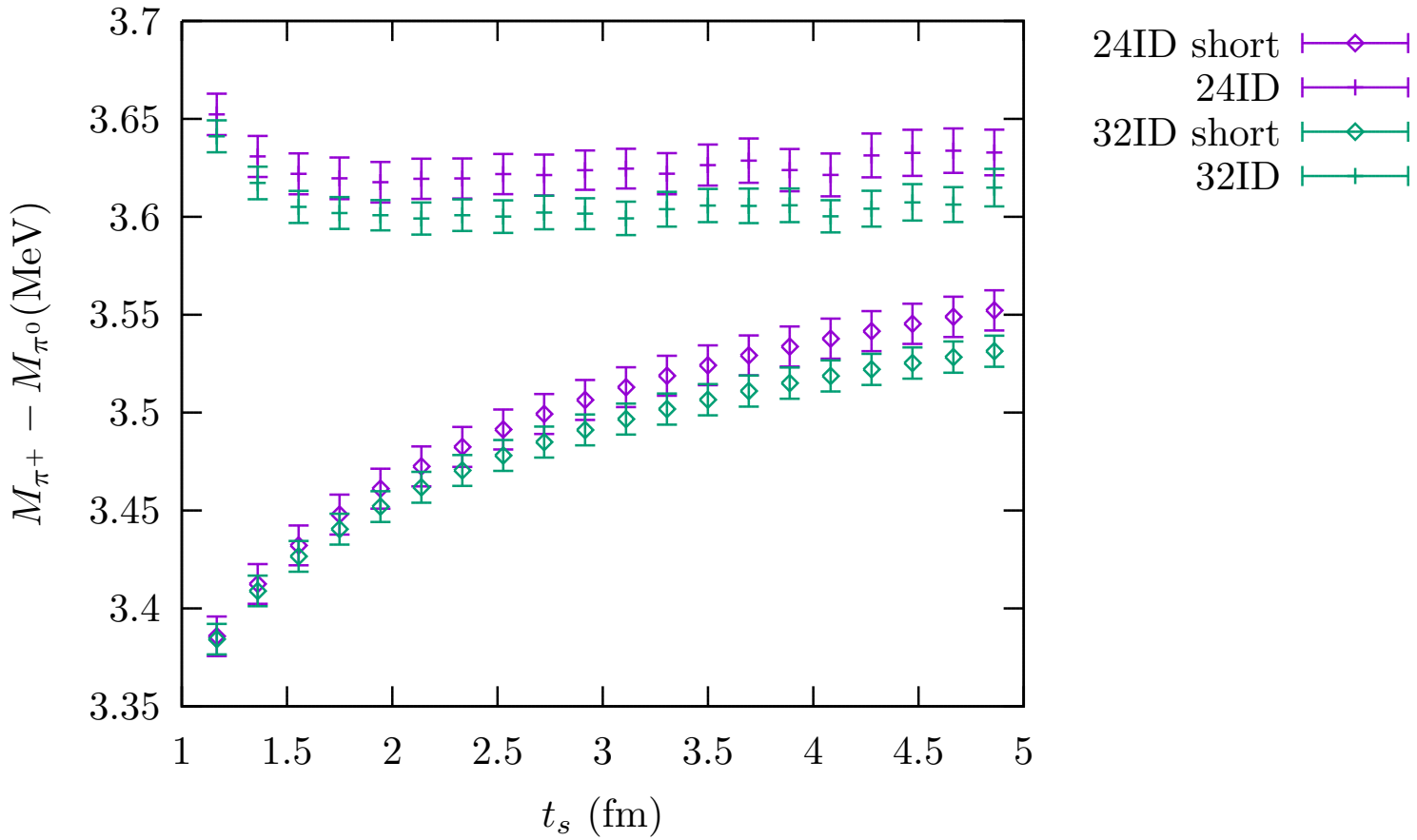

- 24ID: 142 MeV, a^{-1}=1.015 GeV, L=4.7 fm, N_{conf} = 91
- 32ID: 142 MeV, a^{-1}=1.015 GeV, L=6.2 fm, N_{conf} = 56
- ground state saturation at $t_s \gtrsim 1.5$ fm
- stat. error $\lesssim 0.3\%$, including both type 1 and type 2 diagrams
- residual FV effects $\Rightarrow$ $L = 4.7$ fm not large enough for phyiscal m_π

Pion mass splitting

$$\Delta M_\pi^2(a, M_\pi) = \Delta M_\pi^2(0, M_\pi^{\text{phys}}) + c_1 a^2 + c_2 \left(M_\pi^2 - (M_{\pi^+}^{\text{phys}})^2 \right)$$

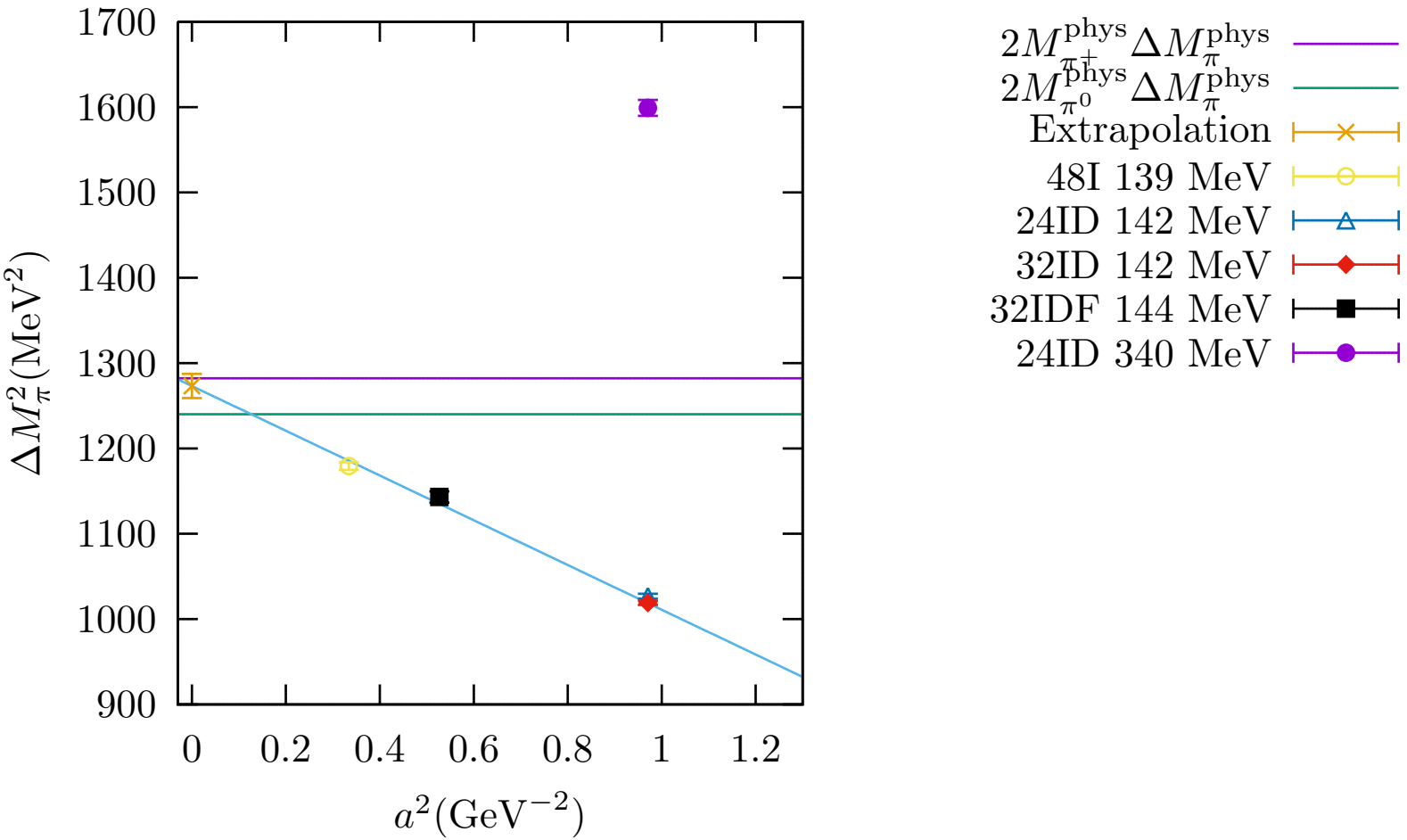

$$\Delta M_\pi^2(0, M_{\pi^+}^{\text{phys}}) = 1.275(15) \times 10^3 \text{ MeV}^2$$

10 times more accurate than previous lattice calculation

Electroweak box diagram

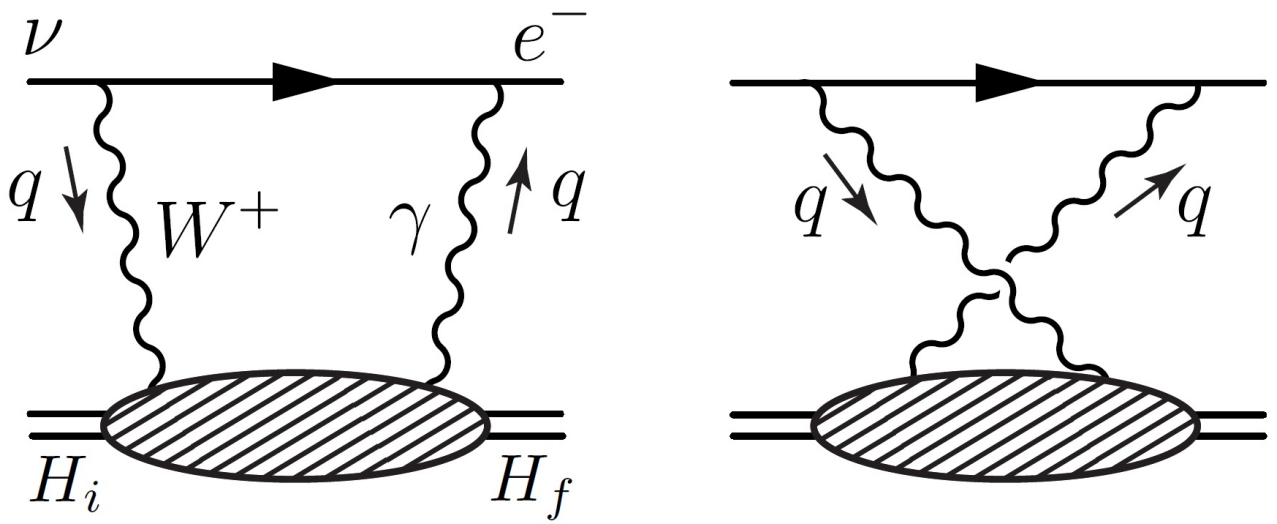

CKM unitarity – a constraint from Standard Model

First-row CKM unitarity

$$\Delta_{\mathrm{CKM}} = |V_{ud}|^2 + |V_{us}|^2 + |V_{ub}|^2 - 1 = 0$$

PDG 2019 ⇒ PDG 2020

	PDG 2019	PDG 2020
$\lvert V_{ud}\rvert$	0.97420(21)	0.97370(14)
$\lvert V_{us}\rvert$	0.2243(5)	0.2245(8)
$\lvert V_{ub}\rvert$	0.00394(36)	0.00382(24)
Δ_{CKM}	−0.00061(47)	−0.00149(45)

- Main update from $|V_{ud}|$ ⇒ 3.3 σ deviation from CKM unitarity
- $|V_{ud}|$ is from superallowed $0^+ \to 0^+$ nuclear beta decay
  - Pure vector transitions at leading order
  - Uncertainty is dominated by electroweak radiative correction

[J. Hardy, I. Towner (2015)]

Axial γW-box diagram

Based on current algebra, only axial γW-box diagram sensitive to hadronic scale

[A. Sirlin, Rev. Mod. Phys. 07 (1978) 573]

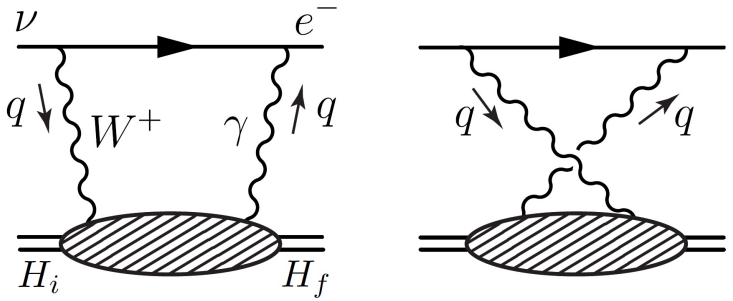

$$T^{VA}_{\mu\nu} = \frac{1}{2}\int d^4x\, e^{iqx}\langle H_f(p)|T\left[J^{em}_{\mu}(x)J^{W,A}_{\nu}(0)\right]|H_i(p)\rangle$$

Re-evaluation of the γW-box diagram

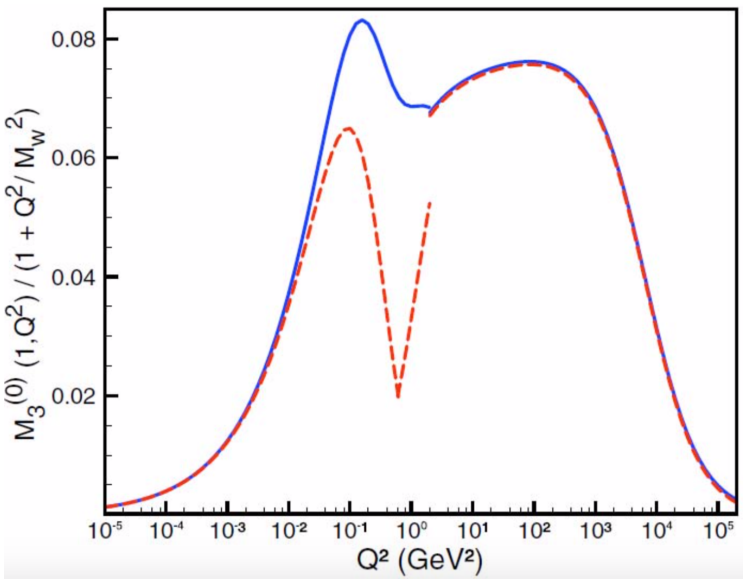

$|V_{ud}| = 0.97420(18)_{\rm RC}(10)_{\mathcal{F}t}$

Using VMD model

[Marciano & Sirlin, PRL 2006]

$\Downarrow$

$|V_{ud}| = 0.97370(10)_{\rm RC}(10)_{\mathcal{F}t}$

Using dispsive & data-driven analysis

[Seng et.al. PRL 2018]

$> 3\sigma$ violation of CKM unitarity $\Rightarrow$ first-principle calculation

Quark contractions for the γW-box diagrams

$$\mathcal{H}^{VA}_{\mu\nu}(x) = \langle \pi^0(p)| T\left[J^{em}_{\mu}(x) J^{W,A}_{\nu}(0)\right] |\pi^-(p)\rangle$$

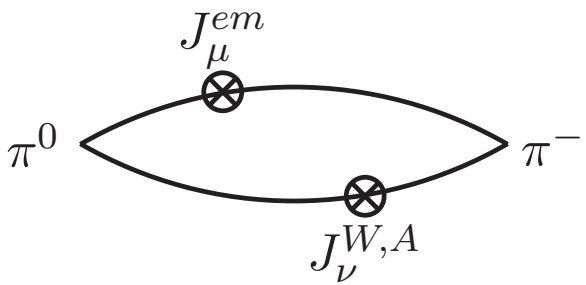

(A)

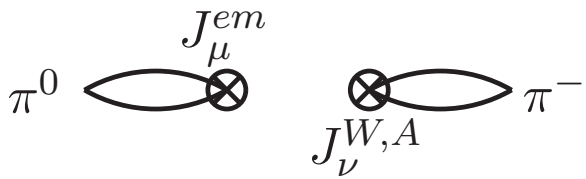

(B)

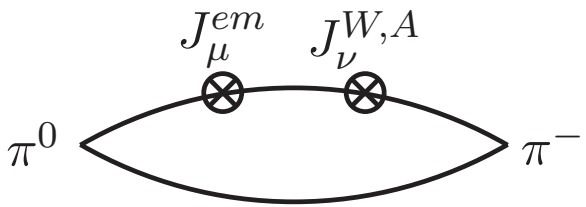

(C)

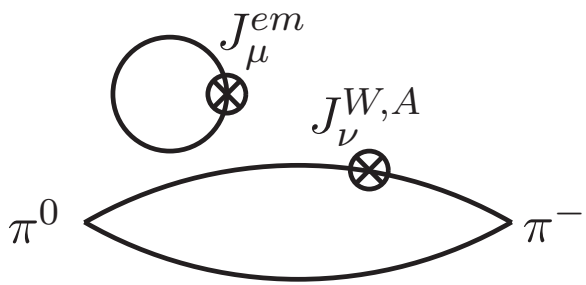

(D)

- Coulomb gauge fixed wall source is used for the pion interpolating field
- FFT is used to perform contraction for diagram (A) and (B)
- Point source propagators are used to compute diagram (C)
- Diagram (D) is suppressed by flavor SU(3) and is neglected

Lattice results for the hadronic functions

Construct the Lorentz scalar function $M_\pi(Q^2)$ from $\mathcal{H}^{VA}_{\mu\nu}(x)$

$$M_\pi(Q^2) = -\frac{1}{6\sqrt{2}} \frac{\sqrt{Q^2}}{m_\pi} \int d^4x\, \omega(Q,x) \epsilon_{\mu\nu\alpha 0} x_\alpha \mathcal{H}^{VA}_{\mu\nu}(x)$$

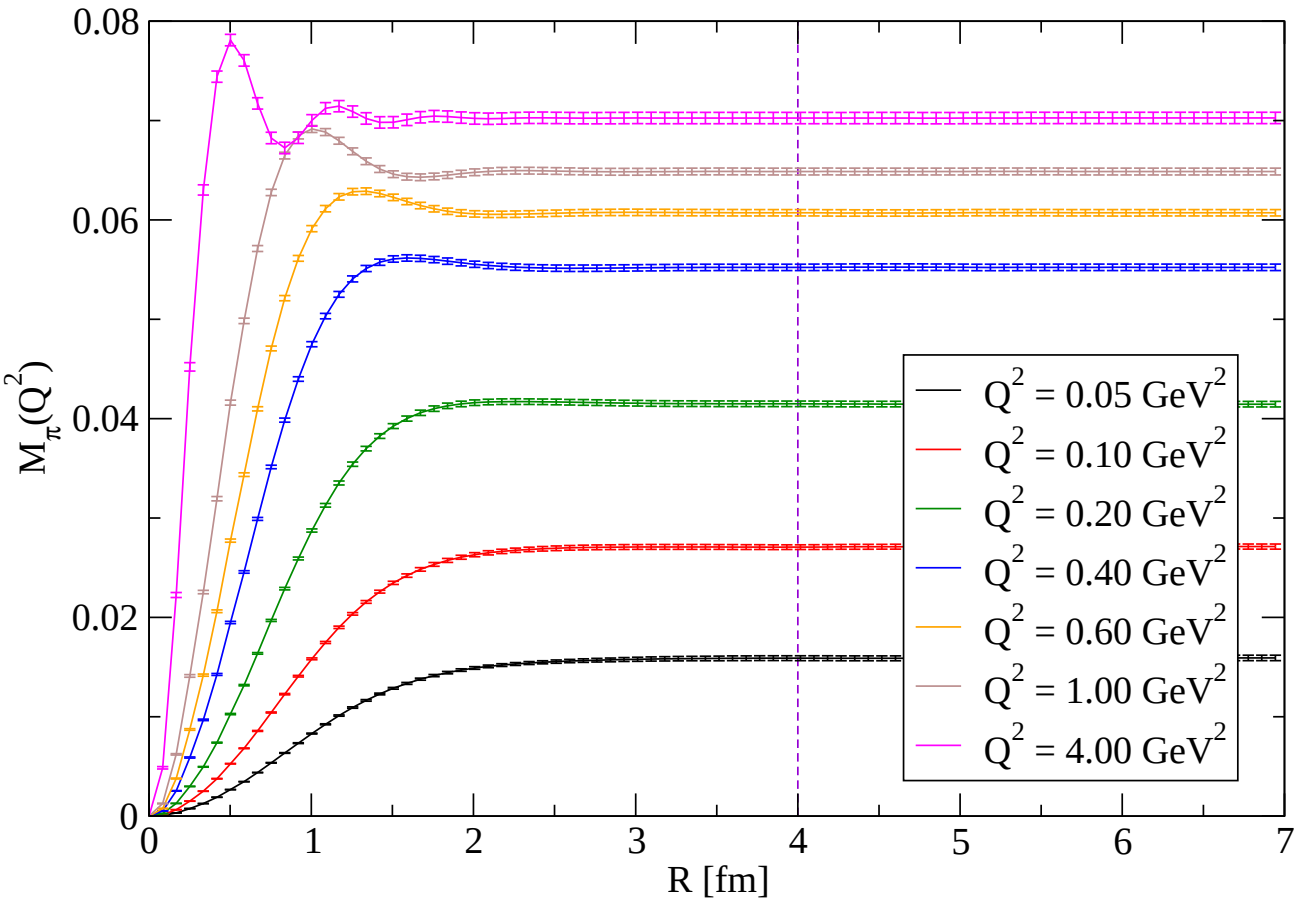

Combine lattice results with pQCD

Radiative correction requires the momentum integral from $0 < Q^2 < \infty$

$$\Box_{\gamma W}^{VA} = \frac{3\alpha_e}{2\pi} \int \frac{dQ^2}{Q^2} \frac{m_W^2}{m_W^2 + Q^2} M_\pi(Q^2)$$

- Lattice data used for low-Q^2 region
- OPE and perturbative Wilson coefficients used for high-Q^2 region

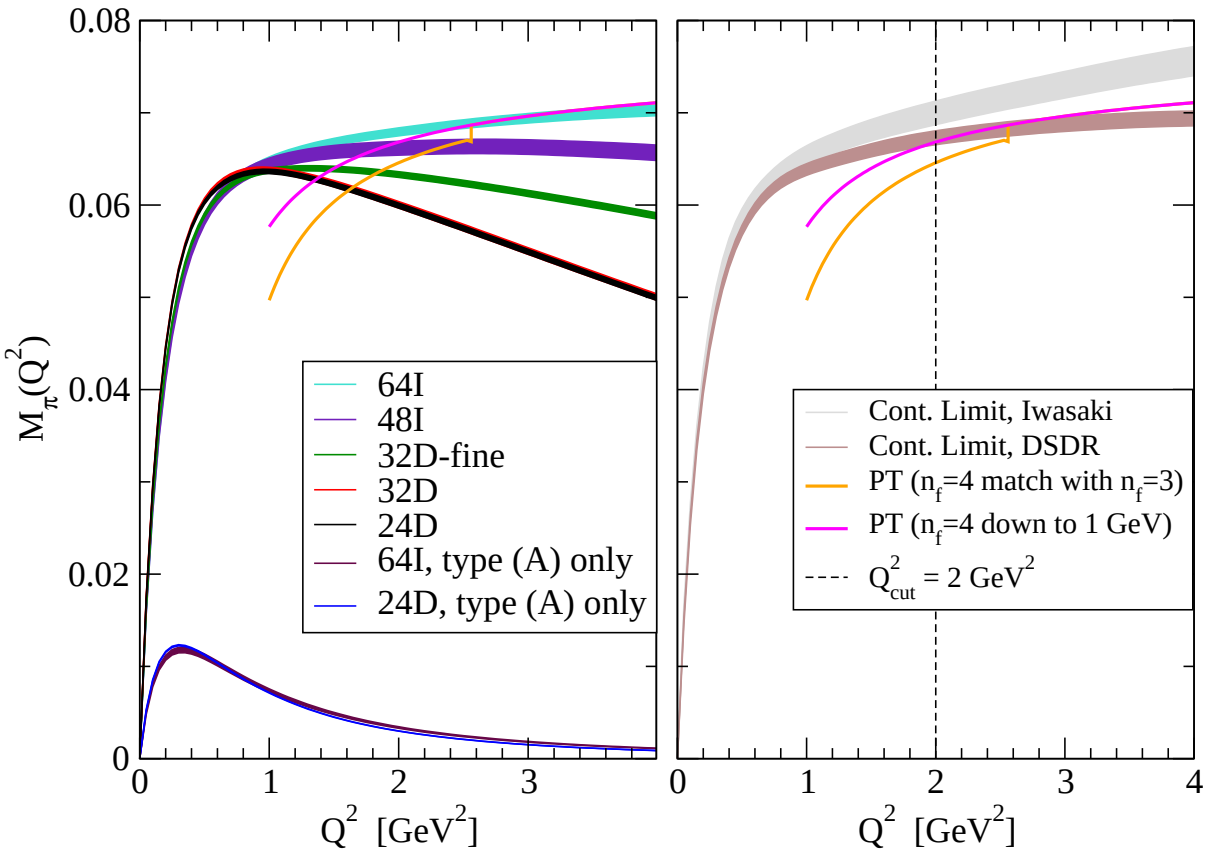

Error analysis

Use the momentum scale $Q^2_{\rm cut}$ to separate the LD and SD contributions

$$\Box^{VA}_{\gamma W} = \begin{cases} 2.816(9)_{\rm stat}(24)_{\rm PT}(18)_{\rm a}(3)_{\rm FV} \times 10^{-3} & \text{using } Q^2_{\rm cut} = 1 \text{ GeV}^2 \\ 2.830(11)_{\rm stat}(9)_{\rm PT}(24)_{\rm a}(3)_{\rm FV} \times 10^{-3} & \text{using } Q^2_{\rm cut} = 2 \text{ GeV}^2 \\ 2.835(12)_{\rm stat}(5)_{\rm PT}(30)_{\rm a}(3)_{\rm FV} \times 10^{-3} & \text{using } Q^2_{\rm cut} = 3 \text{ GeV}^2 \end{cases}$$

- When $Q^2_{\rm cut}$ increase, the lattice artifacts become larger
- When $Q^2_{\rm cut}$ decrease, systematic effects in pQCD become larger
- For 1 GeV$^2 \leq Q^2_{\rm cut} \leq 3$ GeV^2, all results are consistent within uncertainties

Pion semileptonic β decay

Decay width measured by PIBETA experiment

$$\Gamma_{\pi\ell 3} = \frac{G_F^2 |V_{ud}|^2 m_\pi^5 |f_+^\pi(0)|^2}{64\pi^3}(1+\delta) I_\pi$$

- ChPT [Cirigliano et.al. (2002), Czarnecki, Marciano, Sirlin (2019)]

$$\delta = 0.0334(10)_{\rm LEC}(3)_{\rm HO}$$

- Sirlin's parametrization [A. Sirlin, Rev. Mod. Phys. 07 (1978) 573]

$$\begin{aligned}\delta &= \frac{\alpha_e}{2\pi}\left[\bar{g} + 3\ln\frac{m_Z}{m_p} + \ln\frac{M_Z}{M_W} + \tilde{a}_g\right] + \delta_{\rm HO}^{\rm QED} + 2\,\Box_{\gamma W}^{VA} \\ &= 0.0332(1)_{\gamma W}(3)_{\rm HO}\end{aligned}$$

where $\frac{\alpha_e}{2\pi}\bar{g} = 1.051\times 10^{-2}$, $\frac{\alpha_e}{2\pi}\tilde{a}_g = -9.6\times 10^{-5}$, $\delta_{\rm HO}^{\rm QED} = 0.0010(3)$

- Hadronic uncertainty reduced by a factor of 10, which results in

$$|V_{ud}| = 0.9739(28)_{\rm exp}(5)_{\rm th} \quad \Rightarrow \quad |V_{ud}| = 0.9739(28)_{\rm exp}(1)_{\rm th}$$

[XF, Gorchtein, Jin, Ma, Seng, PRL124 (2020) 192002]

First time to calculate γW box diagram $\Rightarrow$ method set up for nucleon decay

$0\nu2\beta$ decays

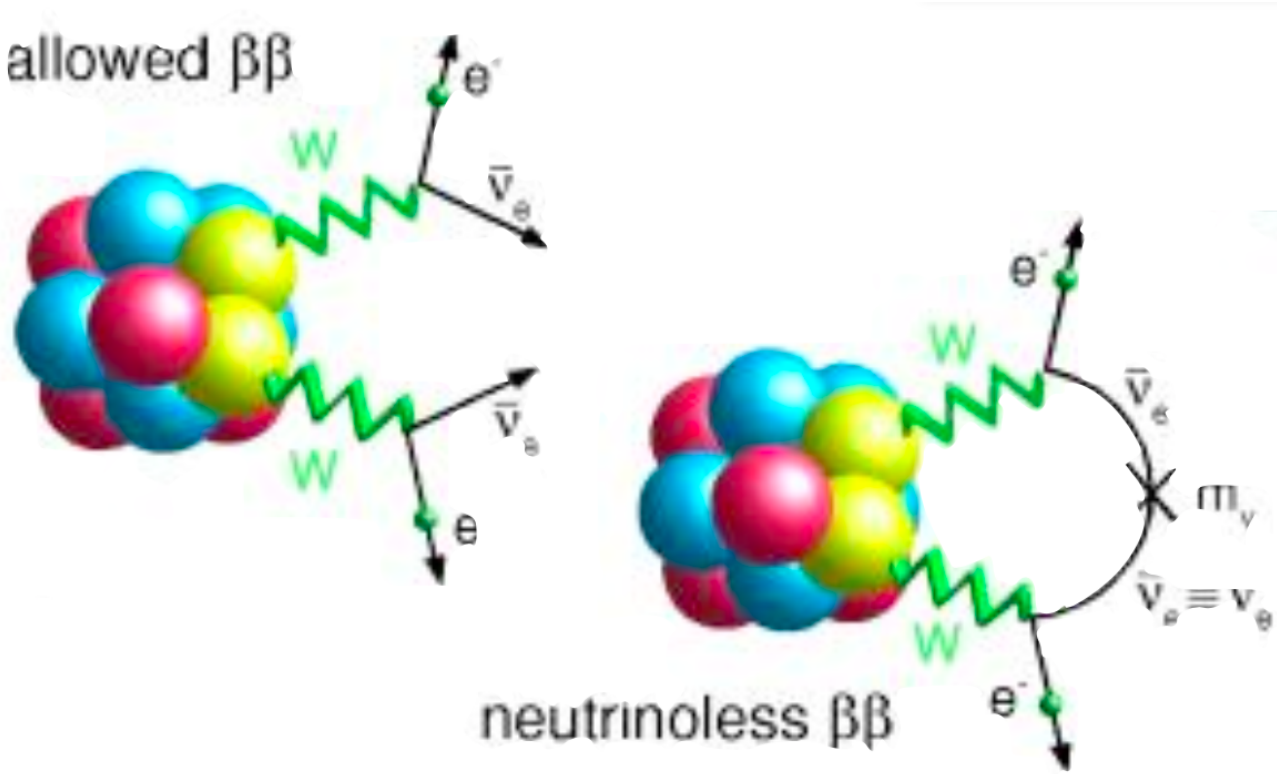

Double beta decays

Early in 1935, Goeppert-Mayer proposed to detect double beta decay

- Nuclear pairing: In some case even-even nucleus is more stable, e.g. Ge^{76}

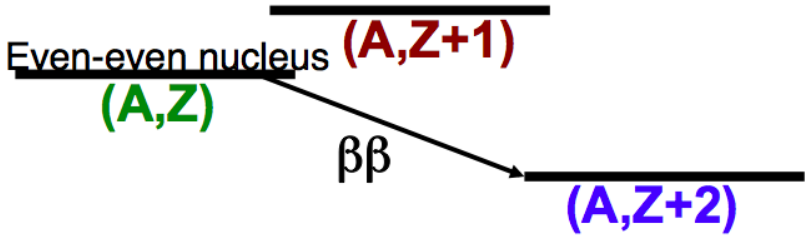

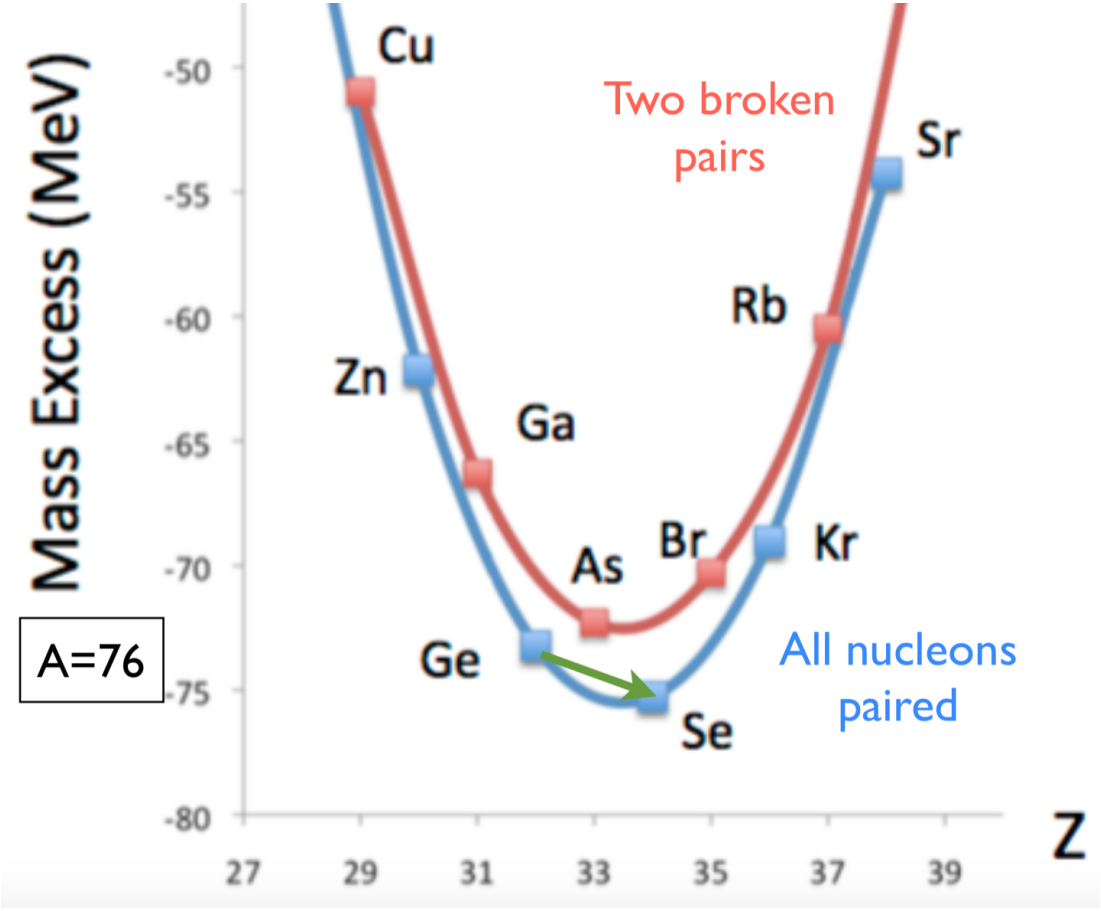

Majorana's proposal in 1937: $\nu = \bar{\nu}$?

$\Leftarrow$ This is allowed by symmetry properties of Dirac's theory

- In single beta decay, one cannot distinguish Dirac or Majorana neutrino
- 1939, Furry propose to search for neutrinoless double beta ($0\nu\beta\beta$) decays

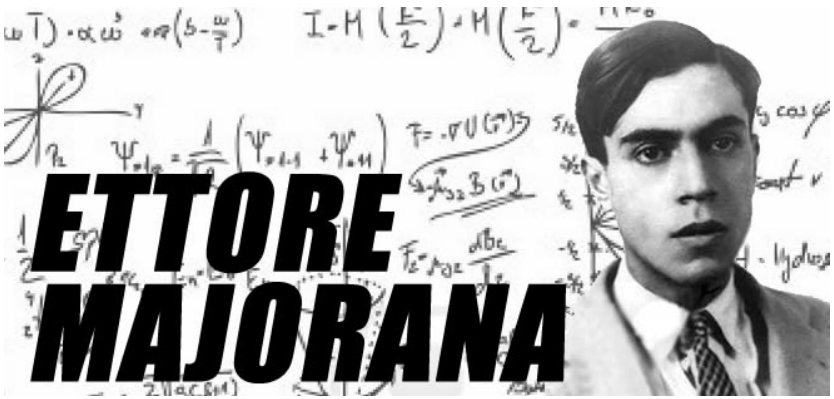

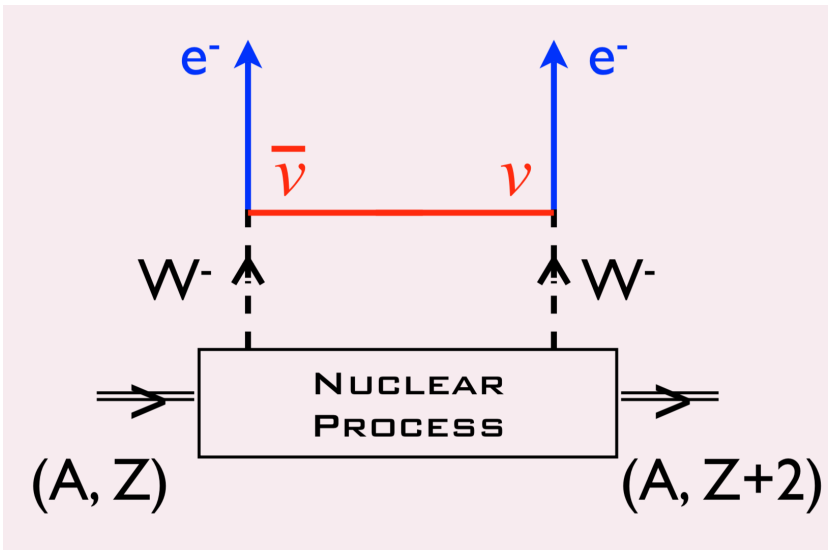

Neutrinos: Majorana or Dirac?

Experiments underway

$0\nu\beta\beta$ decay

- The easiest way to determine whehter ν is a Majorana fermion
- Give the information on the absolute mass scale of ν
- Provide the evidence of lepton number violation

Global experimental search

- 4 Exp. (Majorana, EXO, CUORE, GERDA) reached $T^{0\nu}_{1/2} > 10^{25}$ year
- 1 Exp. (KamLAND-Zen) exceeded the level of 1×10^{26} year

KamLAND-Zen EXO CUORE

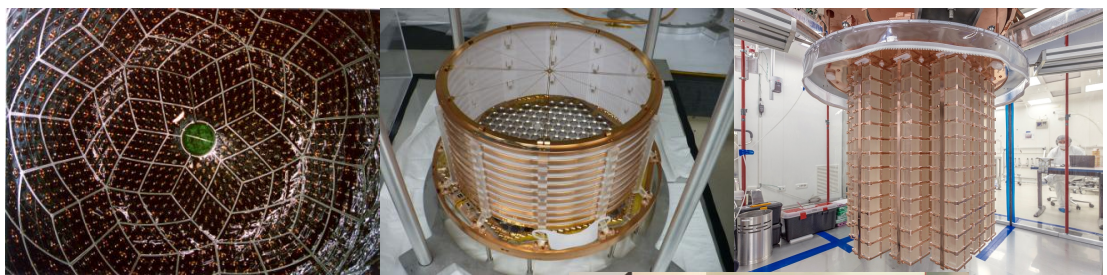

Majorana GERDA

- Jinping underground lab (China) can provide an ideal place for $0\nu2\beta$ search

Chinese experiments join in the international competition

PandaX reports the lower limit of $T^{0\nu}_{1/2} > 2.1 \times 10^{23}$ from Chinese experiments

PandaX 实验组发表首个寻找马约拉纳中微子结果

上海交通大学物理与天文学院 1周前

上海交通大学牵头的PandaX合作组近期在“中国物理C”杂志（IF=5.86）以“编辑推荐”的形式发表了首个利用液氙探测器寻找马约拉纳中微子的实验结果。他们的实验表明，核同位素136Xe通过马约拉纳中微子而产生的衰变寿命大于2.1x1023年， 即两千一百万亿亿年，比宇宙的年龄长了约15万亿倍。这是在中国本土物理实验中探测到最长的核素衰变寿命下限。该结果也能解释为马约拉纳电子中微子有效质量的上限，mee < 1.4~3.7eV/c2(电子伏特)。

Single β decay of nuclei

Coupling of currents to nuclei in nuclear EFT [W. Detmold, talk at Lat18]

- One body coupling dominates

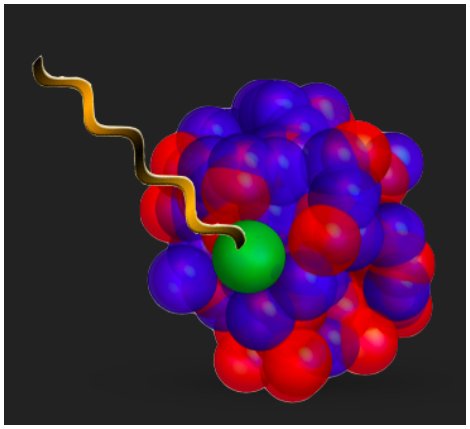

- Two nucleon contributions are subleading but non-negligible

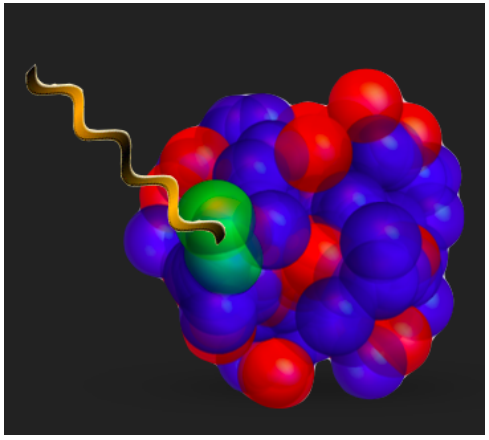

A promising way to provide few-body inputs to ab initio many-body calculations

Progress and Challenges in Neutrinoless Double Beta Decay

ECT* workshop subscription

ECT*, Strada delle Tabarelle, 286, Villazzano, 38123 Trento, Italy

Monday, 15 July 2019 at 08:00 - Friday, 19 July 2019 at 18:00 (CEST)

Summarize on recent advances in

- Lattice QCD
- Chiral effective field theory
- Many-body nuclear theory

Target on

- a seamless connection between the theory at quark and nuclear level
- reliable calculations of the nuclear matrix elements, with robust uncertainty

Exploratory lattice QCD studies

Recent review - Lattice QCD Inputs for Nuclear Double Beta Decay

[Cirigliano, Detmold, Nicholson, Shanahan, 2003.08493]

- $2\nu2\beta$ decay: $nn \to ppee\nu\nu$ @ $m_\pi = 800$ MeV
  [NPLQCD, PRD96 (2017) 054505, PRL119 (2017) 062003]

- $0\nu2\beta$ decays in the pion sector

  - SD contributions in $\langle\pi^+|O_i|\pi^-\rangle$, O_i the local four-quark operators
    [A. Nicholson et al., PRL121 (2018) 172501]
  - LD contributions in $\pi^-\pi^- \to ee$
    [XF, L. Jin, X. Tuo, S. Xia, PRL122 (2019) 022001]
  - LD contributions in $\pi^- \to \pi^+ ee$
    [X. Tuo, XF, L. Jin, PRD100 (2019) 094511]
    [W. Detmold, D. Murphy, arXiv:2004.07404]

$\pi\pi \to ee$ decay amplitude @ $m_\pi = 140$ MeV

XF, L. Jin, X. Tuo, S. Xia, PRL122 (2019) 022001

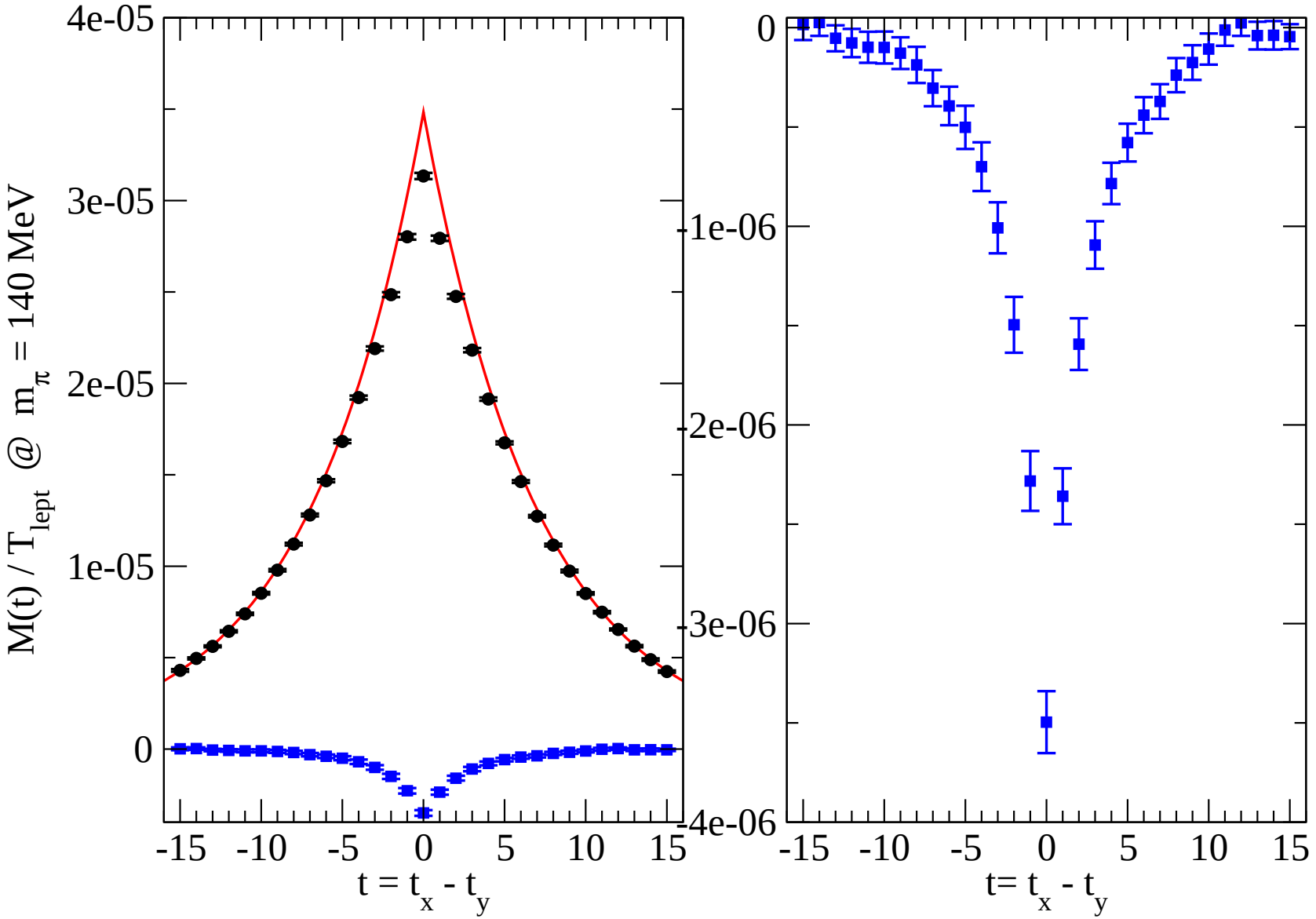

$\pi^- \to \pi^+ ee$: infinite volume reconstruction

X. Tuo, XF, L. Jin, PRD100 (2019) 094511

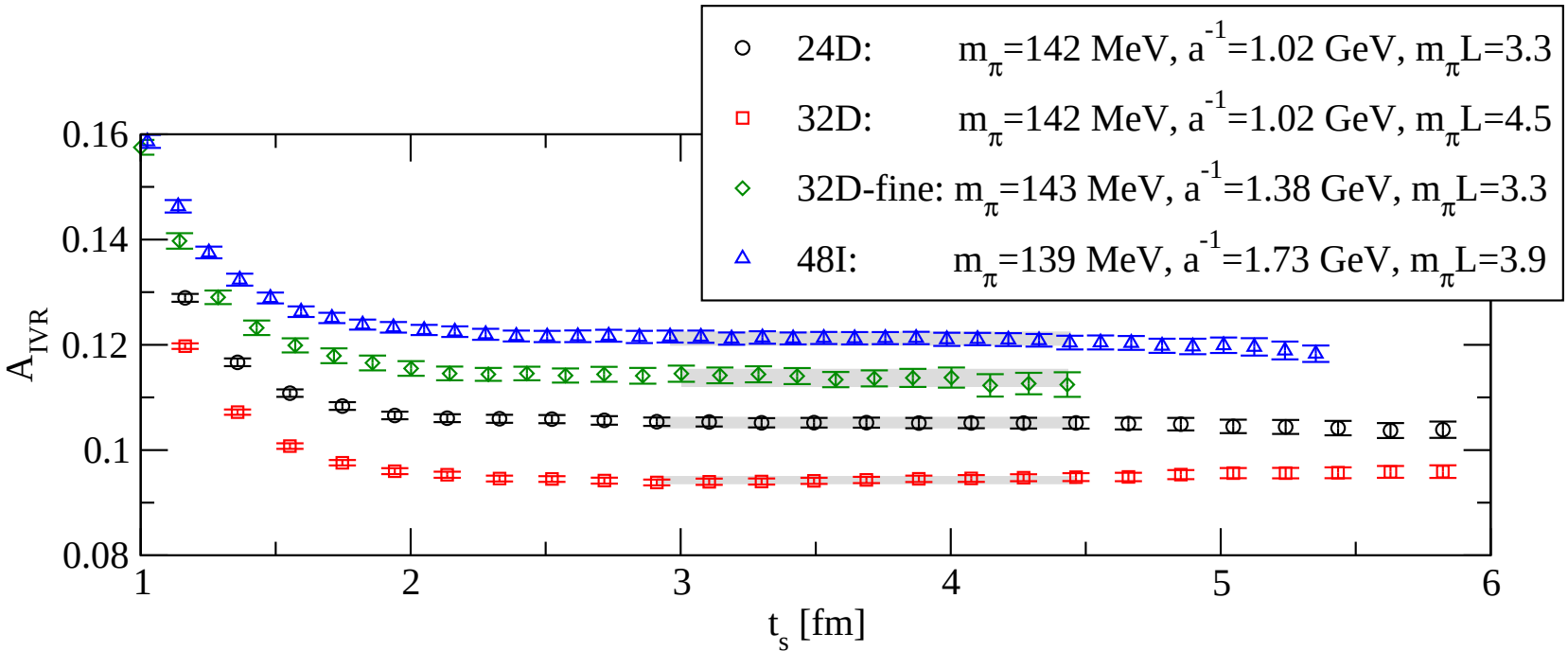

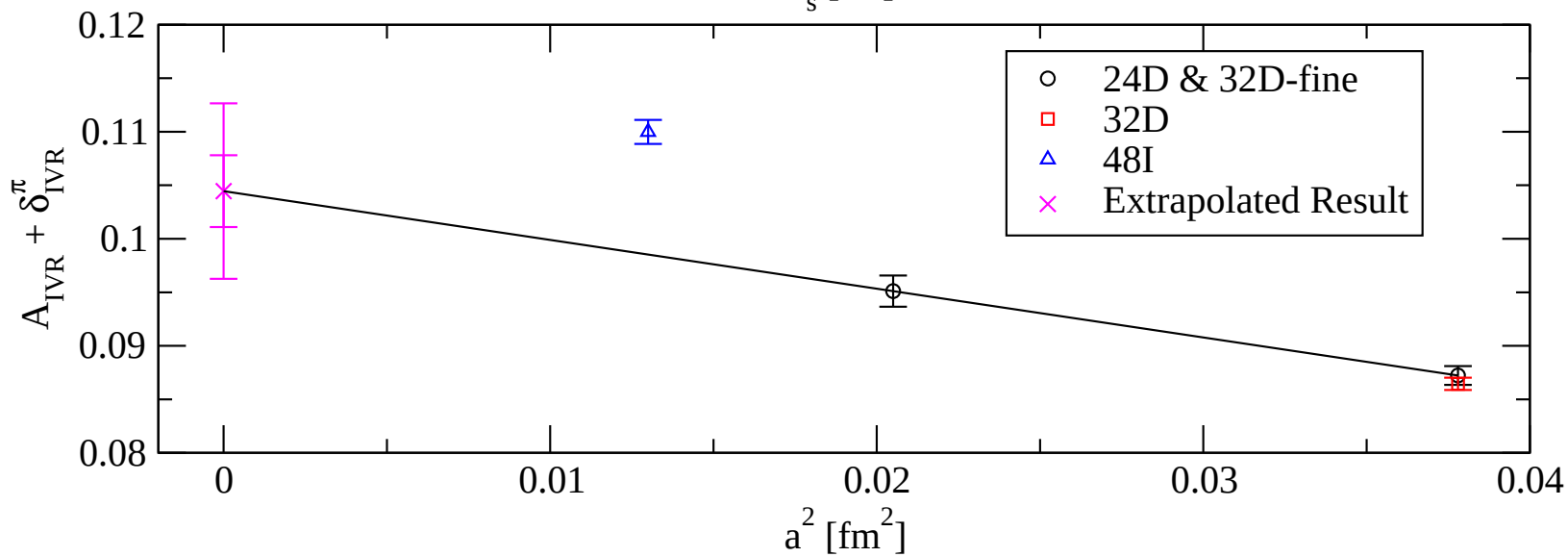

Summary of $\pi^-\pi^- \to ee$ and $\pi^- \to \pi^+ ee$

Chiral perturbation theory for $\pi^-\pi^- \to ee$

[Cirigliano, Dekens, Mereghetti, Walker-Loud, PRC97 (2018) 065501]

$$\frac{\mathcal{A}(\pi^-\pi^- \to ee)}{2F_\pi^2\, T_{\rm lept}} = 1 - \frac{m_\pi^2}{(4\pi F_\pi)^2}\left(3\log\frac{\mu^2}{m_\pi^2} + \frac{7}{2} + \frac{\pi^2}{4} + \frac{5}{6}g_\nu^{\pi\pi}(\mu)\right)$$

Lattice calculation yields (statistical error only)

[XF, L. Jin, X. Tuo, S. Xia, PRL122 (2019) 022001]

$$\frac{\mathcal{A}(\pi\pi \to ee)}{2F_\pi^2\, T_{\rm lept}} = 0.910(3) \quad \Rightarrow \quad g_\nu^{\pi\pi}(m_\rho) = -12.0(3)$$

Chiral perturbation theory for $\pi^- \to \pi^+ ee$

[X. Tuo, XF, L. Jin, PRD100 (2019) 094511]

$$\frac{\mathcal{A}(\pi^- \to \pi^+ ee)}{2F_\pi^2\, T_{\rm lept}} = 1 + \frac{m_\pi^2}{(4\pi F_\pi)^2}\left(3\log\frac{\mu^2}{m_\pi^2} + 6 + \frac{5}{6}g_\nu^{\pi\pi}(\mu)\right)$$

Lattice calculation yields (statistical + systematical errors)

$$\frac{\mathcal{A}(\pi^- \to \pi^+ ee)}{2F_\pi^2\, T_{\rm lept}} = 1.105(3)(7) \quad \Rightarrow \quad g_\nu^{\pi\pi}(m_\rho) = -10.9(3)(7)$$

Also $g_\nu^{\pi\pi}(m_\rho) = -10.8(1)(5)$ [W. Detmold, D. Murphy, arXiv:2004.07404]

Charge radius

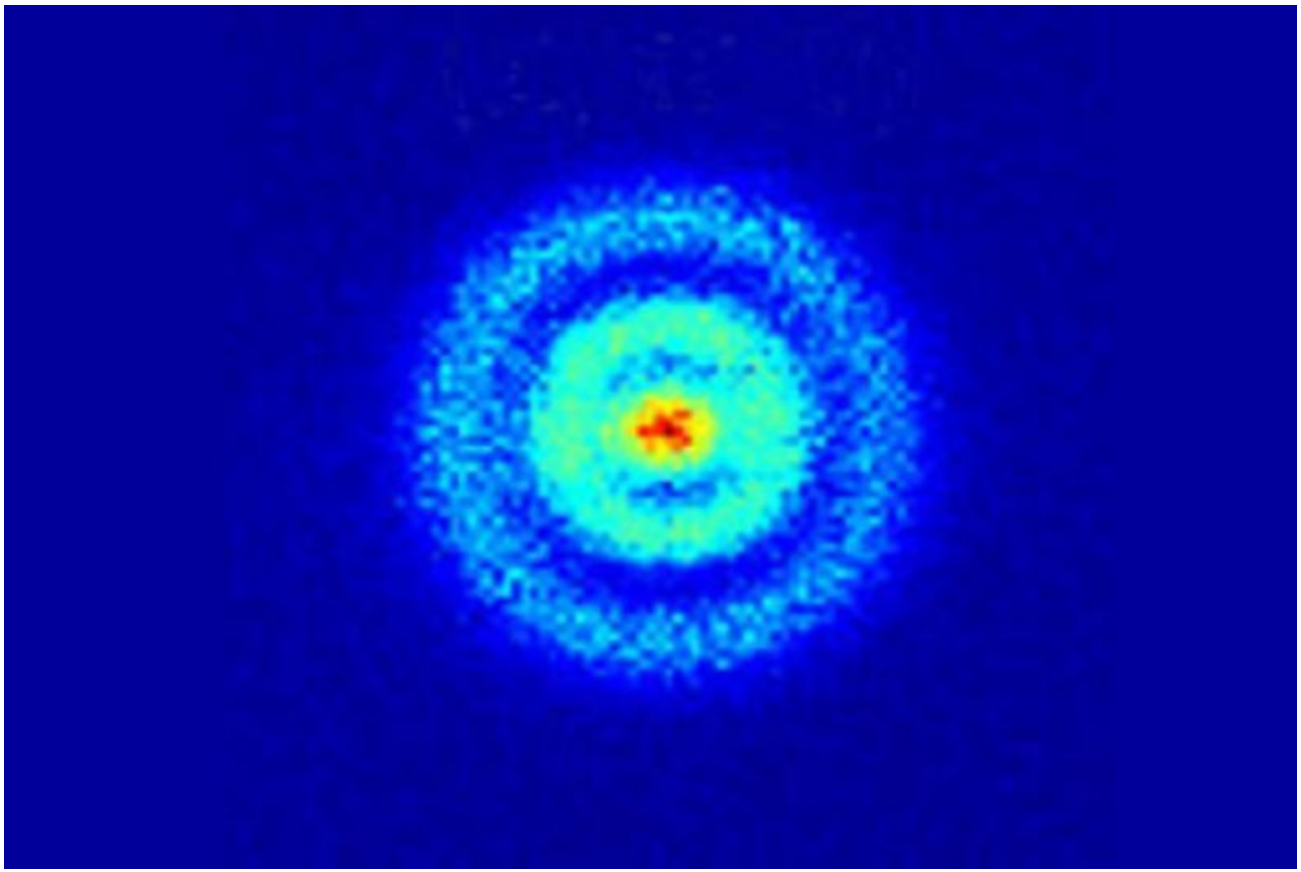

Puzzles of proton size

A decade puzzle since 2010

- Probe charge radius using electron
  - e-p scattering & hydrogen spectrum
  - consistent with uncertainty 0.7%
  - $r_p = 0.8751(61)$ fm
    [Rev. Mod. Phys. 88 (2016) 035009]
- Probe charge radius using muon
  - muonic hydrogen spectrum
  - high precision of uncertainty 0.05%
  - $r_p = 0.84087(39)$ fm
    [Nature 466 (2010) 213]
    [Science 339 (2013) 417]

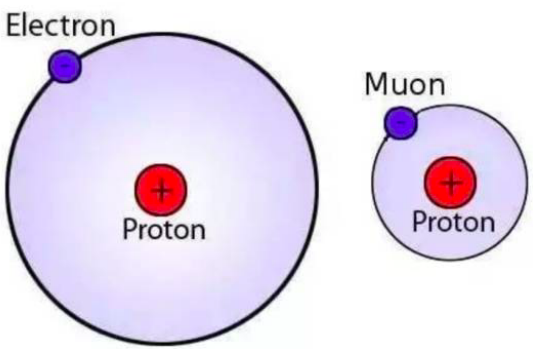

- Muon vs electron, diff by 4%, 5.6σ smaller

Recent progress from experiments

Two very recent "electron" experiments favor smaller charge radius

- Hydrogen spectrum [N. Bezginov, et.al. Science 365 (2019) 1007]
- *e*-*p* scattering [W. Xiong, A. Gasparian, H. Gao, et.al. Nature 575 (2019) 147]

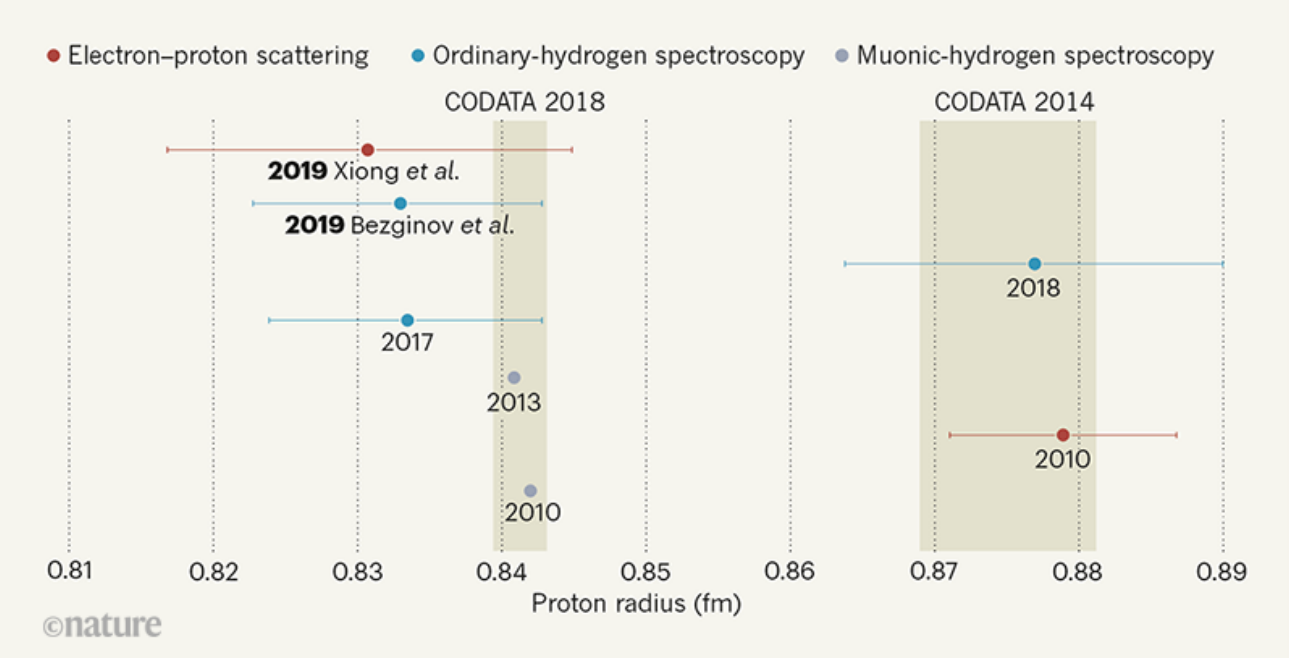

[J.-Ph. Karr & D. Marchand, Nauture 575 (2019) 61-62]

Discrepancy mainly arises from different experiments

Theoretically, lattice QCD can provide the answer to the puzzle

$\Leftarrow$ if various systematic effects are under control

Form factor and charge radius from a static potential

- Consider the scattering of an electron in a potential

$$V(\vec{r}) = \int \frac{Q\rho(\vec{r}')}{4\pi|\vec{r} - \vec{r}'|} d^3\vec{r}'$$

with the charge density

$$\int \rho(\vec{r}) d^3\vec{r} = 1$$

- Transition matrix element for the electron is

$$M_{fi} = \langle \Psi_f | V(\vec{r}) | \Psi_i \rangle = \int e^{-i\vec{p}_f \cdot \vec{r}} V(\vec{r}) e^{i\vec{p}_i \cdot \vec{r}} d^3\vec{r}$$

With the substitution $\vec{R} = \vec{r} - \vec{r}'$ and $\vec{q} = \vec{p}_f - \vec{p}_i$

$$M_{fi} = \int e^{-i\vec{q}\cdot\vec{R}} \frac{Q}{4\pi|\vec{R}|} d^3\vec{R} \int \rho(\vec{r}') e^{-i\vec{q}\cdot\vec{r}'} d^3\vec{r}' = (M_{fi})_{\text{point}} F(\vec{q}^2)$$

- All the information of charge distribution is encoded in the form factor

$$F(\vec{q}^2) = \int \rho(\vec{r}) e^{-i\vec{q}\cdot\vec{r}} d^3\vec{r}$$

- Charge radius is the root of mean squre r^2 under the distribution of $\rho(\vec{r})$

$$\langle r^2 \rangle = \int \rho(\vec{r}) \vec{r}^2 d^3\vec{r} = 6 \frac{dF(\vec{q}^2)}{d\vec{q}^2}\Big|_{q^2=0}$$

Lattice calculation of form factor and charge radius

In QFT, the form factor is given by the matrix element of the EM vector current

$$\langle H(p_f)|J_\mu|H(p_i)\rangle = F(q^2)(p_i+p_f)_\mu, \quad q^2=(p_f-p_i)^2$$

- Momenta p_i and p_f on the lattice are always discrete: $\frac{2\pi}{L}n$
- Requires modeling of the momentum dependence to extract $\langle r^2\rangle$

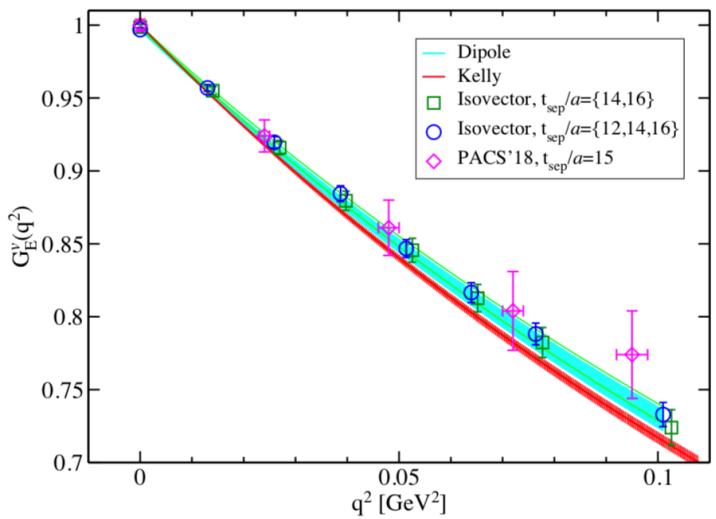

			Isovector	
Fit type	$q^2_{\rm cut}$ [GeV^2]	$t_{\rm sep}/a$	$\sqrt{\langle r_E^2\rangle}$ [fm]	χ^2/dof
Linear	0.013	$\{12,14,16\}$	0.847(23)	–
		$\{14,16\}$	0.885(31)	–
Dipole	0.102	$\{12,14,16\}$	0.875(15)	0.8(6)
		$\{14,16\}$	0.893(24)	0.5(5)
Quadrature	0.102	$\{12,14,16\}$	0.859(17)	0.6(6)
		$\{14,16\}$	0.866(26)	0.7(7)
z-exp ($k_{\rm max}=3$)	0.102	$\{12,14,16\}$	0.862(25)	0.9(8)
		$\{14,16\}$	0.886(33)	0.5(6)

[PACS collab. use a $(10.8\ \text{fm})^4$ lattice, PRD 2019]

- Model depdence could cause a 5% shift in $\langle r^2\rangle$, e.g. 0.847(23)→0.893(24)

Such method has been used for decades ⇒ Any new approach?

Charge radius in the infinite volume

We start with a Euclidean hadronic function in the infinite volume

$$H(x) = \langle 0|A_4(x)J_4(0)|\pi(\vec{0})\rangle, \quad \langle 0|A_4(0)|\pi(p)\rangle = f_\pi E_\pi$$

The spatial Fourier transform of $H(x)$ yields

$$\tilde{H}(t,\vec{p}) \approx \frac{f_\pi}{2}(E_\pi + m_\pi)F_\pi(q^2)e^{-Et}$$

- The derivative of $\tilde{H}(t,\vec{p})$ at $|\vec{p}|^2 = 0$ leads to

$$D(t) \equiv m_\pi^2 \frac{\partial \tilde{H}(t,\vec{p})}{\partial |\vec{p}|^2}\bigg|_{|\vec{p}|^2=0} = -\frac{m_\pi^2}{3!}\int d^3\vec{x}\,|\vec{x}|^2 H(x)$$

  This is very similar as

$$\langle r^2\rangle = \int \rho(\vec{r})\vec{r}^2 d^3\vec{r}$$

- Not difficult to relate $D(t)$ to the charge radius

$$\frac{D(t)}{\tilde{H}(t,\vec{0})} = \frac{1}{4} - \frac{m_\pi t}{2} - c_1, \quad c_1 = \frac{m_\pi^2}{6}\langle r_\pi^2\rangle$$

New method: using $D(t)$ to determine the charge radius

Significant finite-volume effects

$$c_1 = -\frac{D(t)}{\tilde{H}(t,\vec{0})} + \frac{1}{4} - \frac{m_\pi t}{2}$$

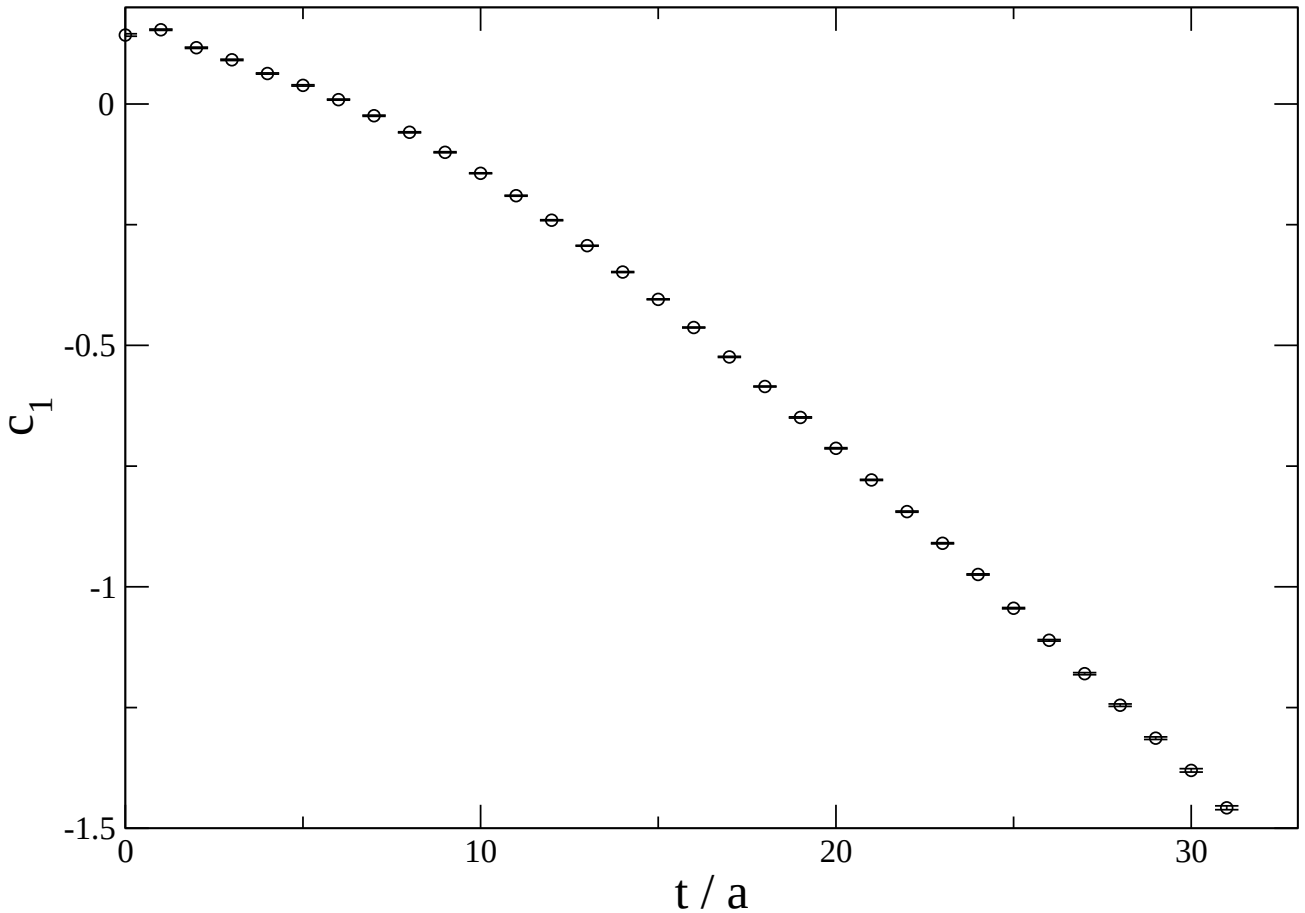

Large finite-volume effects:

$$m_\pi^2 |\vec{x}|^2 H(x) \sim m_\pi^2 |\vec{x}|^2 \exp(-m_\pi \sqrt{\vec{x}^2 + t^2}) \sim 0.53$$

with $\sqrt{\vec{x}^2 + t^2} \approx |\vec{x}| \sim L/2 = 2.5$ fm

Treat with the finite-volume effects properly

From infinite to finite volume

$$\frac{D^{(\infty)}(t)}{\tilde{H}^{(\infty)}(t,\vec{0})} = \frac{1}{4} - \frac{m_\pi t}{2} - c_1 \quad \Rightarrow \quad \frac{D^{(L)}(t)}{\tilde{H}^{(L)}(t,\vec{0})} = \sum_{n=0}^{\infty} \beta_n^{(L)}(t)\, c_n$$

with $\beta_n^{(L)}(t)$ known and $c_n \approx (m_\pi/m_\rho)^{2n}$ suppress quickly as n becomes large

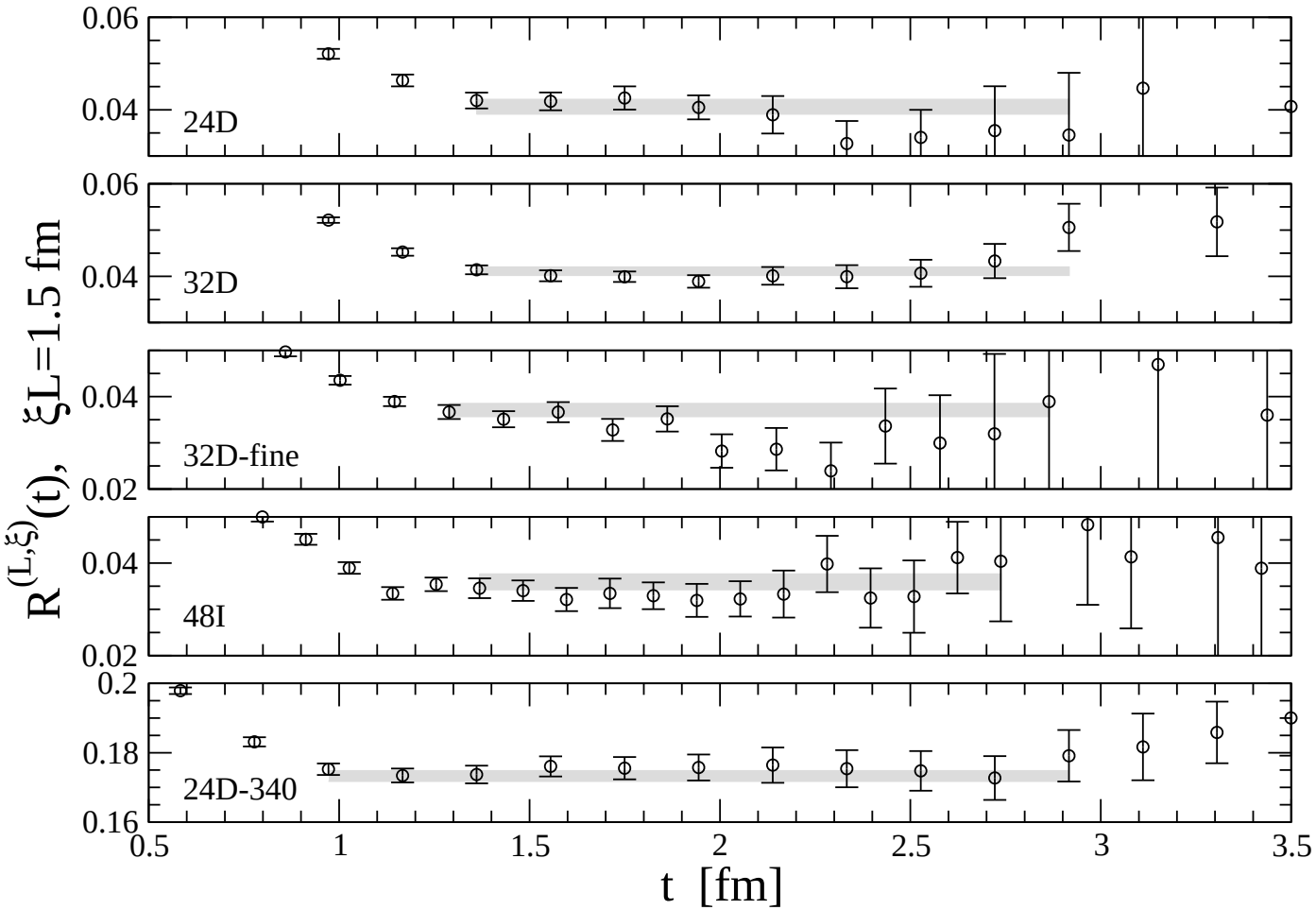

Traditional method

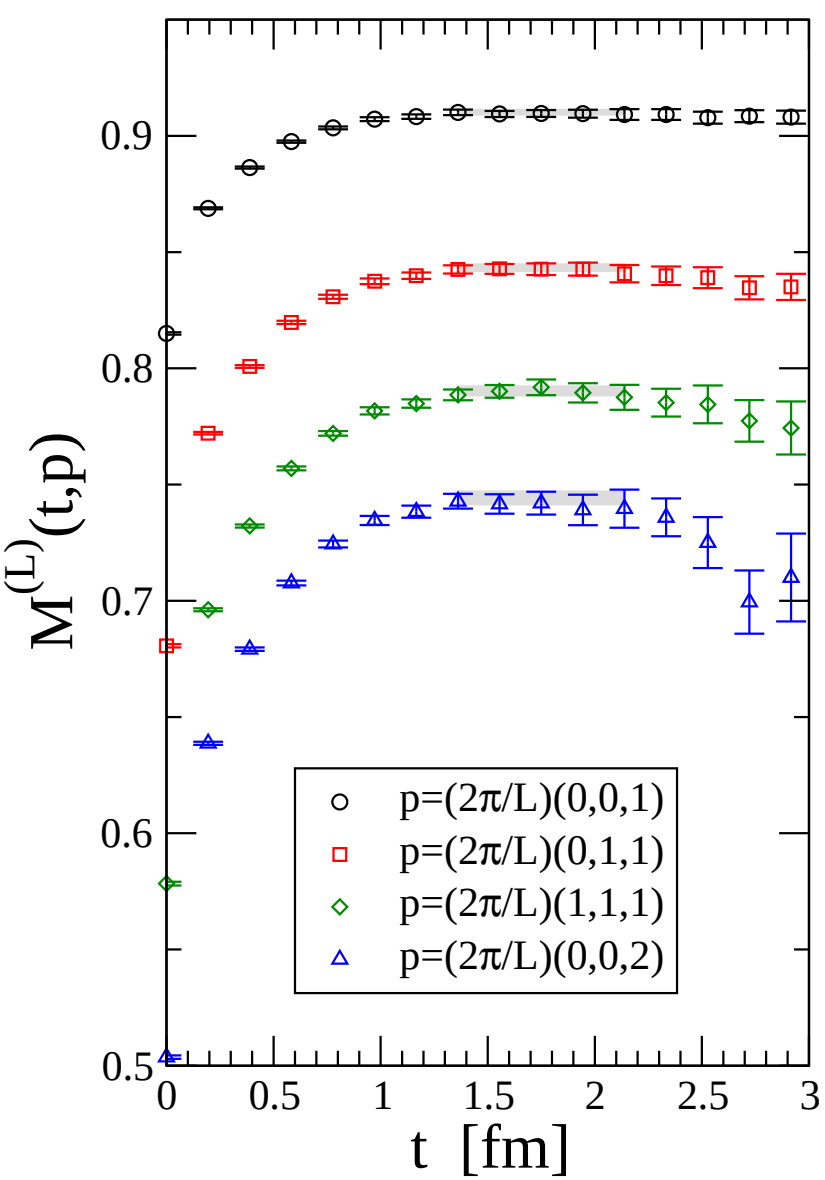

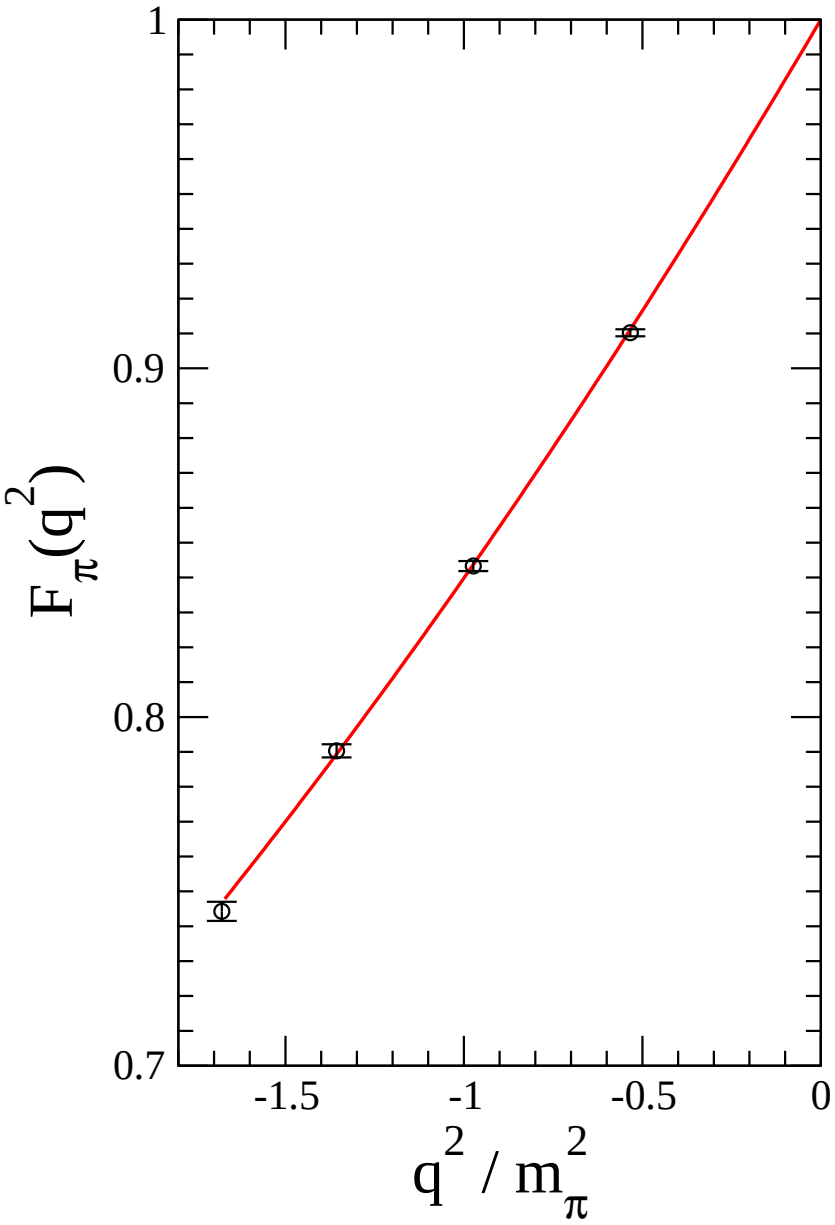

Comparison

[XF, Y. Fu, L. Jin, PRD101 (2020) 051502 (Rapid Communication)]

Ensemble	New	Traditional	
	$\langle r_\pi^2 \rangle$ [fm^2]	$\langle r_\pi^2 \rangle$ [fm^2]	c_V [fm^4]
$m_\pi = 141$ MeV, $a = 0.19$ fm, $L = 4.7$ fm	0.476(18)	0.466(30)	−0.002(2)
$m_\pi = 141$ MeV, $a = 0.19$ fm, $L = 6.2$ fm	0.480(10)	0.479(15)	0.001(1)
$m_\pi = 143$ MeV, $a = 0.14$ fm, $L = 4.6$ fm	0.423(15)	0.409(28)	0.001(2)
$m_\pi = 139$ MeV, $a = 0.11$ fm, $L = 5.5$ fm	0.434(20)	0.395(32)	−0.002(3)
$m_\pi = 341$ MeV, $a = 0.19$ fm, $L = 4.7$ fm	0.3485(27)	0.3495(44)	0.0015(2)
PDG	0.434(5)		

- At $m_\pi \approx 140$ MeV, the statistical errors of $\langle r_\pi^2 \rangle$ range from 2.1% to 4.6%
- At $m_\pi \approx 340$ MeV, the statistical uncertainty is 0.8%
- Final result

  $$\langle r_\pi^2 \rangle = 0.434(20)(13)\ \text{fm}^2$$

  agrees with the PDG value 0.434(5) fm^2

Use this method to explore the puzzle of proton's size

Y. Fu's talk at APLAT 2020 (>300 registered participants)

Lattice QCD calculation of the pion charge radius using a model-independent method

CERTIFICATE *of*

BEST PRESENTATION AWARD

THIS ACKNOWLEDGES THAT

Yang Fu

HAS PRESENTED THE BEST PRESENTATION AT

Asia-Pacific Symposium for
Lattice Field Theory (APLAT 2020)

AUGUST
2020

橋本 省二

Shoji Hashimoto

Chair of the APLAT 2020 Organizing Committee

ANPhA
Asian Nuclear Physics Association

Conclusion

- QCD+QED and pion mass splitting

$$\Delta M_\pi^2 = 1.275(15) \times 10^3 \text{ MeV}^2$$

- Axial γW-box contribution to $\pi_{\ell 3}$ decay

$$\Box_{\gamma W}^{VA} = 2.830(11)_{\text{stat}}(26)_{\text{sys}} \times 10^{-3}$$

- Pion $0\nu 2\beta$ decay

$$\begin{aligned} \pi^-\pi^- \to ee \quad &\Rightarrow \quad g_\nu^{\pi\pi}(m_\rho) = -12.0(3) \\ \pi^- \to \pi^+ ee \quad &\Rightarrow \quad g_\nu^{\pi\pi}(m_\rho) = -10.9(3)(7) \end{aligned}$$

- Pion charge radius

$$\langle r_\pi^2 \rangle = 0.434(20)_{\text{stat}}(13)_{\text{sys}} \text{ fm}^2$$

Move from the pion to the nucleon sector

Outlook

... from **QCD**

via

CHIRAL EFFECTIVE FIELD THEORY ...

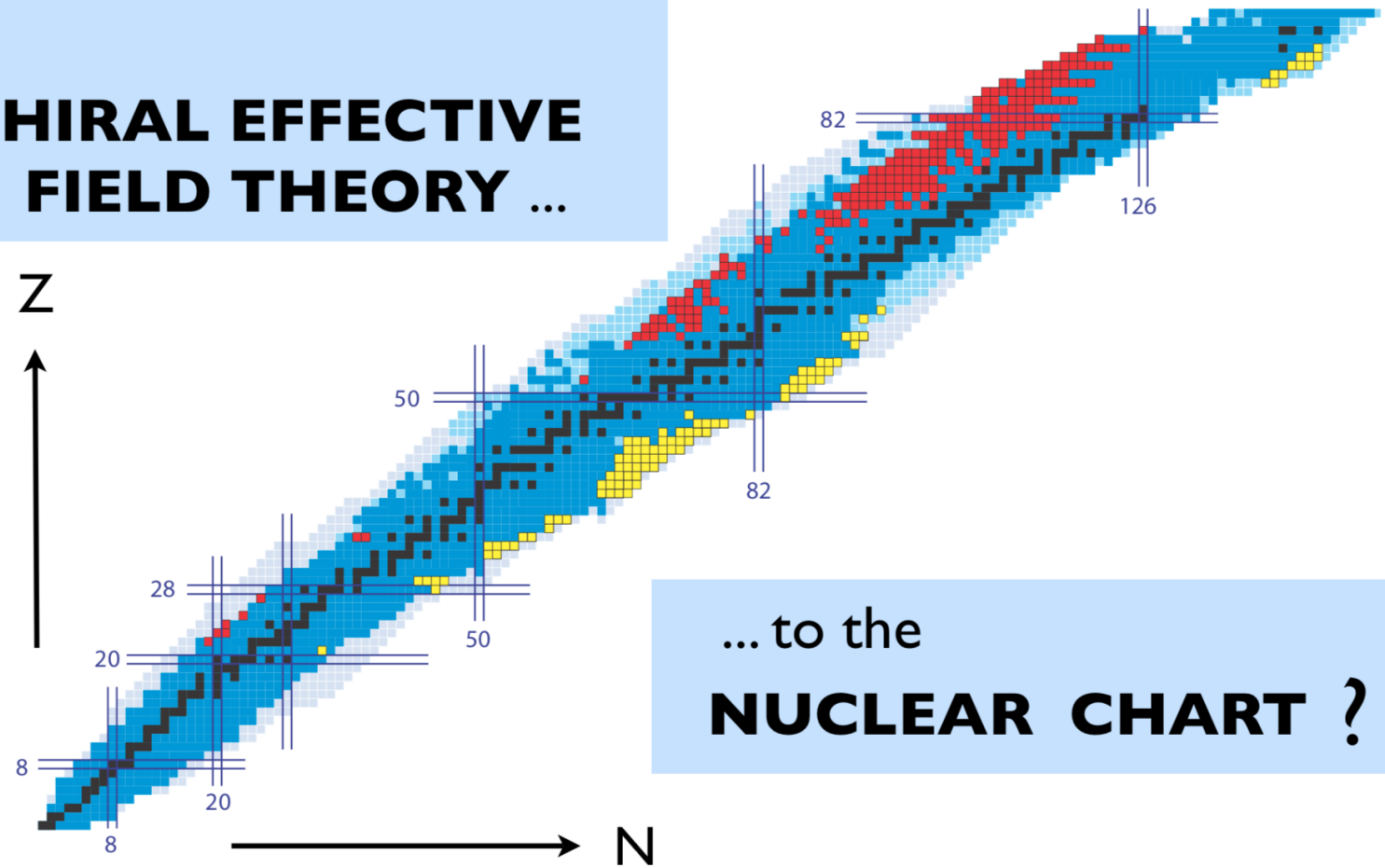

... to the

NUCLEAR CHART ?

Backup slides

Starting from QED$_\infty$

XF, L. Jin, PRD100 (2019) 094509

QED self energy

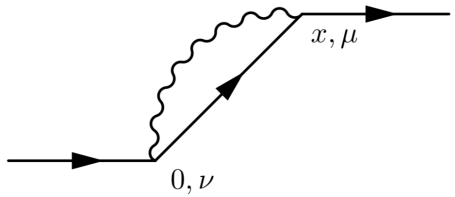

- We start with infinite volume

$$\mathcal{I} = \frac{1}{2} \int d^4x \, \mathcal{H}_{\mu,\nu}(x) S^{\gamma}_{\mu,\nu}(x)$$

where $\mathcal{H}_{\mu,\nu}(x)$ is the hadronic function

$$\mathcal{H}_{\mu,\nu}(x) = \mathcal{H}_{\mu,\nu}(t, \vec{x}) = \langle \pi | T[J_\mu(t, \vec{x}) J_\nu(0)] | \pi \rangle$$

$S^{\gamma}_{\mu,\nu}(x)$ is the photon propagator in the infinite volume

$$S^{\gamma}_{\mu,\nu}(x) = \frac{\delta_{\mu\nu}}{4\pi^2 x^2}$$

- Propose to replace $\mathcal{H}_{\mu,\nu}(x)$ by $\mathcal{H}^{\text{lat}}_{\mu,\nu}(x)$

However, this still leads to power-law FV effects

Analysis of hadronic function

XF, L. Jin, PRD100 (2019) 094509

- We have proposed to replace $\mathcal{H}_{\mu,\nu}(x)$ by $\mathcal{H}^{\rm lat}_{\mu,\nu}(x)$
  - $\mathcal{H}^{\rm lat}_{\mu,\nu}(x)$ mainly differs from $\mathcal{H}_{\mu,\nu}(x)$ at the boundry of the box: $x \sim L$
- The hadronic part $\mathcal{H}_{\mu,\nu}(x)$ is given by

$$\mathcal{H}_{\mu,\nu}(x) = \mathcal{H}_{\mu,\nu}(t,\vec{x}) = \langle\pi|T[J_\mu(t,\vec{x})J_\nu(0)]|\pi\rangle$$

  - $J_\mu(t,\vec{x})J_\nu(0) \quad \to \quad e^{-M_\pi\sqrt{t^2+\vec{x}}} \quad \Rightarrow \quad$ exp. suppressed
  - $\langle\pi|J_\mu(t,\vec{x}) \quad \to \quad e^{M_\pi t} \quad \Rightarrow \quad$ exp. enhanced

For small $|t|$, we have exponentially suppressed FV effects:

$\mathcal{H}_{\mu,\nu}(t,\vec{x}) \sim e^{-M\left(\sqrt{t^2+\vec{x}^2}-t\right)} \sim e^{-M|\vec{x}|} \quad \Rightarrow \quad$ Exponentially suppressed FV effects

For large $|t|$, we shall have:

$\mathcal{H}_{\mu,\nu}(t,\vec{x}) \sim e^{-M_\pi\left(\sqrt{t^2+\vec{x}^2}-t\right)} \sim e^{-M_\pi\frac{\vec{x}^2}{2t}} \sim O(1) \quad \Rightarrow \quad$ Pow-law suppressed FV effects

Infinite volume reconstruction method

XF, L. Jin, PRD100 (2019) 094509

Realizing at large $t > t_s$ we have ground state dominance:

$$\langle P|J_\mu(t,\vec{x})J_\nu(0)|P\rangle \sim \int \frac{d^3\vec{k}}{(2\pi)^3}\langle P|J_\mu(0)|P(\vec{k})\rangle\langle P(\vec{k})|J_\nu(0)|P\rangle e^{-E_{\vec{k}}t+Mt}e^{-i\vec{k}\cdot\vec{x}}$$

- Reconstruct $\mathcal{H}_{\mu,\nu}(t,\vec{x})$ at large t using $\mathcal{H}_{\mu,\nu}(t_s,\vec{x})$ at modest t_s

$$\mathcal{H}_{\mu,\nu}(t,\vec{x}') \approx \int d^3\vec{x}\,\mathcal{H}_{\mu,\nu}(t_s,\vec{x})\int \frac{d^3\vec{k}}{(2\pi)^3}e^{i\vec{k}\cdot\vec{x}}e^{-(E_{\vec{k}}-M)(t-t_s)}e^{-i\vec{p}\cdot\vec{x}'}$$

Replace

$$\mathcal{H}_{\mu,\nu}(t,\vec{x}) \quad \Leftarrow \quad \mathcal{H}_{\mu,\nu}(t_s,\vec{x}) \quad \Leftarrow \quad \mathcal{H}^{\rm lat}_{\mu,\nu}(t_s,\vec{x})$$

The replacement only amounts for exponentially suppressed FV effects